



## ISTITUTO NAZIONALE DI RICERCA METROLOGICA Repository Istituzionale

Quantum imaging with sub-Poissonian light: challenges and perspectives in optical metrology

*Original*

Quantum imaging with sub-Poissonian light: challenges and perspectives in optical metrology / Ruo Berchera, I; Degiovanni, Ip. - In: METROLOGIA. - ISSN 0026-1394. - 56:2(2019), p. 024001. [10.1088/1681-7575/aaf7b2]

*Availability:*

This version is available at: 11696/59915 since: 2021-02-01T10:49:12Z

*Publisher:*

IOP SCIENCE

*Published*

DOI:10.1088/1681-7575/aaf7b2

*Terms of use:*

This article is made available under terms and conditions as specified in the corresponding bibliographic description in the repository

*Publisher copyright*

(Article begins on next page)

PAPER • OPEN ACCESS

# Quantum imaging with sub-Poissonian light: challenges and perspectives in optical metrology

To cite this article: I Ruo Berchera and I P Degiovanni 2019 *Metrologia* **56** 024001

View the [article online](#) for updates and enhancements.

# Quantum imaging with sub-Poissonian light: challenges and perspectives in optical metrology

I Ruo Berchera and I P Degiovanni

INRIM, Strada delle Cacce 91, I-10135 Torino, Italy

E-mail: [i.ruoberchera@inrim.it](mailto:i.ruoberchera@inrim.it)

Received 8 August 2018, revised 30 November 2018

Accepted for publication 11 December 2018

Published 25 January 2019



## Abstract

Non-classical correlations in optical beams offer an unprecedented opportunity for surpassing the conventional limits of sensitivity and resolution in optical measurements and imaging, especially, but not only, when low photon flux, down to the single photon, is measured. We review the principles of quantum imaging and sensing techniques that exploit sub-Poissonian photon statistics and non-classical photon number correlation, presenting some state-of-the-art achievements in the field. These quantum photonics protocols have the potential to trigger major steps in many applications, such as microscopy and biophotonics, and represent an important opportunity for a new deal in radiometry and photometry.

Keywords: quantum imaging, quantum correlations, quantum metrology, quantum enhanced measurement, quantum optics

(Some figures may appear in colour only in the online journal)

## 1. Introduction

The technological exploitation of quantum states and quantum correlations, aiming to overcome the limits of conventional systems [1], is one of the most, if not the most, active research frontier nowadays. Scientists, from all areas, are committed to applying these new paradigms to different physical platforms, from atomic systems to solid state and photonic devices [2]. A tremendous scientific impact, ranging from biology and medicine to fundamental physics, and extraordinary technological advancement, ranging from communication and computation to precision sensing, is expected in few years or in a near future perspective. Quantum optics and quantum photonics are rather mature in this sense, including several technologies already having potential market diffusion, such as e.g. quantum key distribution [3].

In particular, quantum metrology, one of the main pillars of quantum technologies, has recently been demonstrated to improve

the sensitivity of some of the most sophisticated optical instruments currently available [4], i.e. large scale interferometers for gravitational waves detection, otherwise limited by photon shot-noise. Other examples of promising quantum enhanced measurement techniques have been developed for particle tracking in optical tweezers [5], in sub-shot-noise wide field microscopy [6], quantum correlated imaging [7] and spectroscopy [8], displacement measurement [9], and remote detection and ranging [10].

In this process, the metrology community has a double role. On one side, the development of quantum technology needs a metrological infrastructure for the characterisation of the quantum photonics devices, and for their certification. This requires a knowledge of the basic principles of the quantum strategy, expertise in the sources characterisation (e.g. their photon number statistics, the squeezing or sub-shot-noise properties, up to entanglement quantification), and in the operation of single- or few-photon detectors. On the other side, optical metrology has the opportunity to exploit the peculiar properties of quantum light to develop more accurate measurement, imaging and sensing techniques [11, 12].



Original content from this work may be used under the terms of the [Creative Commons Attribution 3.0 licence](https://creativecommons.org/licenses/by/3.0/). Any further distribution of this work must maintain attribution to the author(s) and the title of the work, journal citation and DOI.

The process has already started: for example, a heralded single-photon source has been successfully applied to the calibration of single-photon detectors by metrologists [13], and similar quantum technique has been extended to detectors for low photon fluxes [14, 15].

Of particular interest, from the radiometric point of view, is the possibility of developing absolute light sources with sub-shot-noise performance, since the shot-noise level becomes a serious limitation to the uncertainty reduction in measurements performed in the few-photon regime. Probing and imaging delicate systems using a small number of photons with true and significant sensitivity improvement would be extraordinarily important, for instance in biological and biochemical investigation [16]. In addition, there are biological effects that are triggered by a single photon, like retina phototransduction [17]. Thus, the quantum measurement strategy presented here, can also be considered the precursors of a potentially brand new metrological research field, namely quantum photometry.

In section 2, we first present the fundamental limits of conventional (classical) optical measurements and imaging techniques, in particular the diffraction limit (DL) and the shot-noise limit (SNL). Then, in section 3 we describe the properties of quantum states sources, such as the single-photon source, Fock states and twin-beam, which, by virtue of their non-classical photon statistics and correlations allow surpassing classical limits. A certain number of quantum imaging techniques, their advantages and their limitations, are presented in section 4. In section 5, we discuss single-photon metrology for new directions in vision research and photometry. Short- and mid-term perspectives in (quantum) optical metrology and conclusions are drawn in section 6.

## 2. Limits of classical (conventional) imaging

Measuring changes in intensity or in phase of an electromagnetic field, after interacting with matter, is the most simple way to extract relevant information on the properties of a system under investigation, whether a biological sample [18] or a digital memory disc [19].

The term ‘imaging’ usually (not always) refers to the reconstruction of the whole spatial properties of the sample, namely in 2D or 3D, and it can be achieved in two different modalities, wide-field or point-by-point scanning. Wide field imaging is preferable in many cases, since it provides a more complete dynamic picture but, for a static sample, the point-by-point scanning offers advantages, for example better  $z$ -resolution in confocal microscopy.

In any case, the two parameters quantifying the quality (the amount of information) of the image are the resolution, i.e. the minimum distance at which two points can be distinguished, and the sensitivity, i.e. the minimum measurable variation of the quantity of interest in a certain point.

The quality of an image is always affected by several limitations, some of them avoidable by careful design of the experiment (aberration, background, artefacts), others imposed by technical limitations of the available actual technology (for instance unavoidable noise or low efficiency of the detector),

and others related to more fundamental reasons. In particular the diffraction limit and the shot-noise limit represent ‘fundamental’ bounds to resolution and sensitivity, at least when classical states of light are considered. A possibility to overcome these limitations is offered by peculiar properties of quantum light.

### 2.1. Diffraction limit (DL)

The DL,  $R \simeq 0.61\lambda/NA$  (with  $\lambda$  being the wavelength of the light and  $NA$  the numerical aperture of the imaging system), represents the maximum obtainable imaging resolution in classical far-field imaging/microscopy. Depending on the kind of light radiation involved, namely incoherent or coherent, it takes the name of Abbe or Rayleigh diffraction limit, respectively.

The DL provides a lower bound to the current capability of precisely measuring the position of objects, from the small one such as e.g. single-photon emitters (colour centres, quantum dots, etc) [20–24], to distant stars. In general, the research of methods to obtain imaging and microscopy resolution below the diffraction limit is a topic of the utmost interest [25–31] that could provide dramatic improvement in the observation of several systems spanning from quantum dots to living cells [5, 32–35], to distant astronomical objects. As a notable example, in several entanglement-related experiments using strongly coupled single-photon emitters it is of the utmost importance to measure their positions with the highest spatial resolution. In principle, this limitation is overcome in microscopy by recently developed techniques such as e.g. stimulated emission depletion (STED) and ground state depletion (GSD) [36, 37], leading their inventors to win the Nobel Prize in 2014. Nevertheless, even if they have been demonstrated to effectively provide super-resolved imaging in a lot of specific applications, including colour centres in diamond [38], they are characterised by rather specific experimental requirements (dual laser excitation system, availability of luminescence quenching mechanisms by stimulated emission, non-trivial shaping of the quenching beam, high power).

In this paper we will focus more on proposal and experiments of sub-diffraction imaging techniques exploiting the peculiar properties of quantum light, rather the ones connected to structured light and individually addressed or quenched fluorophores.

### 2.2. Shot-noise limit (SNL)

The sensitivity bound is established by the laws of quantum mechanics [39–42] and is related to the mean energy of the probe beam. In particular, in standard imaging and sensing exploiting classical probes, the sensitivity is fundamentally lower bounded by the SNL,  $U_{\text{SNL}} \sim \langle N_P \rangle^{-1/2}$ , where  $\langle N_P \rangle$  is the mean number of photons in the probe.

Since the definition of classicality is not univocal, here we intend as ‘classical states’ those providing experimental outcomes that would be completely explainable within the semi-classical theory of photodetection, in which the light is treated

as a electromagnetic wave and the photocurrent is discrete, being a flow of electrons [43]. In the semiclassical picture, the probability of promoting an electron in the conduction band in a infinitesimal time interval is proportional to the light intensity. As a consequence, a plane wave with constant intensity in macroscopic time interval generates  $n_e$  photo-electrons following a Poissonian probability distribution  $P(n_e)$ .

Indeed, in quantum mechanics a plane wave with constant intensity is represented by a coherent state of the form:

$$|\beta\rangle = e^{|\beta|^2/2} \sum_{n=0}^{\infty} \frac{\beta^n}{\sqrt{n!}} |n\rangle, \quad (1)$$

with Poissonian photon number statistics  $P(n) = |\langle \hat{n} | \beta \rangle|^2 = e^{-\langle \hat{n} \rangle} \frac{\langle \hat{n} \rangle^n}{n!}$ , which reproduces the observed photocurrent by the absorption of a photon and the excitation of a photo-electron. All the states that can be represented as a statistical mixture of coherent states, in Glauber–Sudarshan form

$$\rho = \int d^2\beta P(\beta) |\beta\rangle \langle \beta|, \text{ with } P(\beta) \geq 0, \quad (2)$$

are ‘classical’ according to the definition conventionally used in quantum optics [44]. It is easy to show that these states must have Poissonian (or super-Poissonian) photon number fluctuation, with photon-number variance  $\langle \Delta^2 \hat{n} \rangle$  equal (or larger) to the mean photon number, i.e.  $\langle \Delta^2 \hat{n} \rangle \geq \langle \hat{n} \rangle$ .

By contrast, the detection of sub-Poissonian variance,  $\langle \Delta^2 \hat{n} \rangle < \langle \hat{n} \rangle$ , is sufficient to indicate the non-classical nature of the light, according to the quantum optics definition.

In order to study the photon statistics influence on the optical measurement, let us consider the problem of absorption estimation. Sending a probe beam with mean number of photon  $\langle \hat{n} \rangle$  through a sample with absorption factor  $\alpha$ , and measuring the beam mean power after the interaction one gets  $\langle \hat{n}' \rangle = (1 - \alpha) \langle \hat{n} \rangle$ , see figure 1(a). The uncertainty on the absorption it is simply given by:

$$\Delta\alpha = \frac{\sqrt{\langle \Delta^2 \hat{n}' \rangle}}{\left| \frac{\partial \langle \hat{n}' \rangle}{\partial \alpha} \right|}. \quad (3)$$

If the probe statistics is Poissonian, immediately one obtains  $\Delta\alpha_{\text{SNL}} = [(1 - \alpha)/\langle \hat{n} \rangle]^{1/2}$ , graphically represented by the red line in figure 1(b). Thus, it is clear how the SNL is related to the Poissonian fluctuation in classical states of light.

The phase estimation problem can be treated similarly. The output power of a Mach Zehnder or a Michelson interferometer is  $\langle \hat{n}' \rangle = \tau \langle \hat{n} \rangle$ , where  $\tau$  depends on the phase shift  $\phi$  among the arms,  $\tau = \sin^2(\phi/2)$ . Using the uncertainty propagation on equation (3) where  $\phi$  is placed instead of  $\alpha$ , and assuming Poissonian statistics of the light, one gets  $\Delta\phi = \langle \hat{n} \rangle^{-1/2} \cos(\phi/2)^{-1}$ . For  $\phi = 0$  it reaches the lowest value, which is again the SNL.

Such classical limits in loss and phase estimations that we have found here by assuming a specific and simple detection strategy and Poissonian light, coincide with the ultimate bounds achievable by a coherent state and the most general measurement allowed by quantum mechanics: see [42, 45, 46] for loss estimation and [39, 40, 47] for phase estimation.

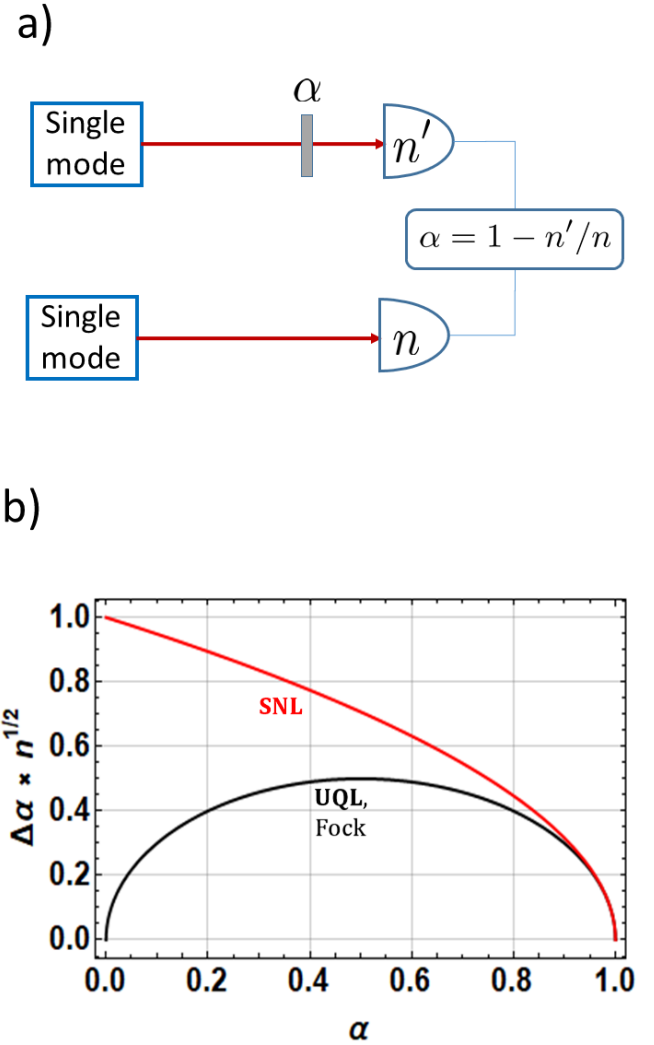


**Figure 1.** Loss estimation. (a) The loss estimation is obtained by comparing the number of photons detected with and without the absorbing sample. (b) Uncertainty in function of the loss parameter  $\alpha$ . SNL stands for shot-noise limit, while UQL stands for ultimate quantum limit.

Of course, increasing arbitrarily the number of photons, i.e. the optical power, one can always reduce the shot-noise contribution to the uncertainty budget below other technical noise. However, this is not always an option. Beating such a limit is particularly important when there are optical power constraints. In addition to fundamental problems related to quantum back-action [47], there are several practical situations in which one may need to limit the optical power.

- *Extremely precise measurements.* In the last generation of a gravitational wave detector the power circulating in the interferometer is of the order of 1 kW (CW), about  $10^{21}$  photon  $s^{-1}$ . This allows reaching the sensitivity in the strain of  $\Delta h < 10^{-22}$  Hz $^{-1/2}$ . A further increasing of the power would have thermal effects on the surface of the mirrors and other optical components, producing an unwanted large scattering interfering with beam propagation.
- *Probing delicate systems (biological sample, photosensitive chemicals).* Damage due to optical tweezers has been



reported for *Escherichia coli*, *Listeria* and other bacteria. Alteration of chemical and biological photosensitive processes can occur at very low power.

- *Investigate response of a system at few photons level.* Some biophysical and biochemical processes, for example phototransduction in vision, or photosynthesis are triggered by the absorption of one or few photons. Moreover, the development of quantum technologies are strongly based on single- or few-photon state manipulation and detection. In order to study and calibrate a single-photon detector, or the retina response at the few-photons level, it is fundamental to develop sub-shot-noise techniques.
- *Developing standards and traceable measurements at the few-photons/single-photon level.* The need for dedicated metrology tools in the few-photon regime is one of the keys to success of quantum photonics technologies (quantum cryptography, quantum sensing and imaging). On the other hand, new insights into the study of the retinal process and response at low light levels are a strong motivation for the development of quantum photometry.

### 3. Beyond classical limits using quantum states

One can note that the conventional statistical scaling of the uncertainty after  $N$  independent repetitions of the same measurement coincides with the scaling of the SNL when  $N$  photons are detected,  $N^{-1/2}$ . This means that photons in classical states behave somehow independently of each other, which results in Poissonian behaviour. However, quantum mechanics does not prevent light beams from having sub-Poissonian fluctuations, or more generally a strong degree of cooperation among photons, where the probability of detecting a photon at a certain time  $t$  is correlated or anti-correlated to the detection of a photon at time  $t_0$ . An ordinate and pseudo-deterministic stream of photons, such as produced by single-photon sources, and pairs of correlated beams named ‘twin beam’ (TWB) can now be ordinarily generated.

For the sake of completeness, aside from sub-Poissonian statistics, there are other way to define the ‘quantumness’ of a state, the most important of them is the concept of entanglement. The state of a system composed by two (or more) subsystems, for example a pair of particles, is entangled *if and only if* it cannot be written in terms of the product state of each individual subsystem. The entanglement implies the existence of a degree of correlation among the particles that cannot be explained in any realistic and local theory [48]. It has been definitely verified that in an entangled state, the measurement of a particle influences the results of the measurement on the other particle, even if they are space-like separated, i.e. causally disconnected [49, 50], revealing the existence of that kind of ‘spooky action at a distance’ in the words of Einstein [51].

Most theoretical investigations in quantum metrology have been addressed to improving the scaling of the uncertainty with the photon number exploiting entanglement, up to the ultimate limit imposed by quantum mechanics,  $N^{-1}$ , known as the Heisenberg limit. For a large photon number, Heisenberg scaling would bring enormous advantages and many schemes

have been proposed [52–55], typically using the entangled state of the form  $2^{-1/2}(|n_A 0_B\rangle + |0_A n_B\rangle)$  (NOON state). This state is a quantum coherent superposition of two possibilities: either the  $n$  photons pass all in the arm  $A$  of an interferometer or they travel all in the arm  $B$ . A phase shift  $\varphi$  acting on the arm  $A$  introduces a global phase difference  $n\varphi$  among the two possibilities of the superposition. Combining at a beam splitter (BS) the two modes  $A$  and  $B$  give  $n$ -times denser interference fringes,  $\sin^2(n\varphi)$ , reaching the Heisenberg scaling of the sensitivity. Unfortunately, while two-photon entangled states can be routinely produced by photon pairs emitted in spontaneous parametric down conversion (SPDC) and the Hong Ou–Mandel effect (described in section 3.2), generation and detection of entangled states with a larger number of photons, i.e.  $n > 4$ , is extremely challenging.

Even worse, entanglement itself is extremely fragile to losses, for example losing a single photon from a NOON state projects it into a classical mixture. A real advantage is preserved only if  $\eta^n v^2 > 1$ , where  $\eta$  is the detection efficiency and  $v$  the visibility of the interference [56]; this condition becomes harder and harder to fulfil with increasing photon number  $n$ . Other quantum states, entangled and squeezed, which are more resilient to experimental imperfections [57], have been considered, but nevertheless reaching the Heisenberg limit for a large number of photons is probably a chimera. In fact, recently it has been shown that in the presence of decoherence the Heisenberg limit, and in general any chance of the uncertainty scaling with the photon number, is out of reach [58, 59]. Rather, the enhancement with respect to the standard quantum limit is given by a constant factor, for example it takes the form  $\sqrt{(1-\eta)/\eta}$  in the presence of a loss factor  $(1-\eta)$  [60].

Nevertheless, the possibility of generating entangled states (such as NOON states with  $N = 2$ ) and the availability of single-photon detectors have enabled the demonstration of the quantum state potentiality in super-resolved lithography [29, 61], phase contrast polarisation microscopy [62, 63], magnetic field sensing [64] and solution concentration measurement [65].

On the other hand, quantum advantages can be obtained more easily by exploiting non-classical Gaussian states [66], which are relatively easy to be produced experimentally, such as a squeezed vacuum generated by SPDC and optical parametric oscillators (OPOs). Single-mode squeezing [67, 68] in one of the quadratures (generated by OPO) that was the first quantum property considered in quantum metrology, in particular for quantum enhanced interferometry [69], has also been more successful from the practical point of view, leading to a real sensitivity improvement of the modern gravitational wave detectors [68, 70]. It leads also to promising application in photonic force microscopy for biological particle tracking [5, 71] and beam displacement measurement [9, 72].

In the context of this paper it is useful to dwell on how the optical losses modify the light properties. In quantum optics loss mechanisms are usually described by the action of a BS with transmittance  $\tau$  and reflectance  $1 - \tau$ , having the field of interest entering one of the input ports of the BS and the

‘vacuum’ entering the other port. The linear unitary evolution leads to the following statistics of the transmitted photon number  $n'$ , in function of the input one  $n$ :

$$\begin{aligned}\langle \hat{n}' \rangle &= \tau \langle \hat{n} \rangle \\ \langle \Delta^2 \hat{n}' \rangle &= \tau^2 \langle \Delta^2 \hat{n} \rangle + \tau(1 - \tau) \langle \hat{n} \rangle.\end{aligned}\quad (4)$$

Note that, in the presence of losses, photon statistics always contain a shot-noise contribution, the one proportional to the mean value of input photons, regardless of the input variance. This can be seen as the effect of the vacuum fluctuation at the unused port of the BS. From equation (4), it is clear that a Poissonian fluctuation in input,  $\langle \Delta^2 \hat{n} \rangle = \langle \hat{n} \rangle$ , remains Poissonian just by a rescaling of the mean photon number. The thermal light (black-body), which has super-Poissonian statistics such as  $\langle \Delta^2 \hat{n} \rangle = \langle \hat{n} \rangle(1 + \langle \hat{n} \rangle)$ , remains unchanged too.

By contrast, losses negatively affect the sub-Poissonian character of light, e.g. Fock states  $|n\rangle$ , eigenstates of the photon number operator, having (by definition) zero-fluctuation  $\langle \Delta^2 \hat{n} \rangle = 0$ , have as output statistic in the presence of losses  $\langle \Delta^2 \hat{n}' \rangle = \tau(1 - \tau) \langle \hat{n} \rangle$ , which approaches the Poissonian one for  $\tau \ll 1$ .

In section 2.2 we derived the uncertainty in loss estimation in the case of Poissonian light. Now, substituting the quantities of equation (4) in the uncertainty expression in equation (3) (with  $\tau = 1 - \alpha$ ) we can derive the more general expression:

$$\Delta\alpha = \sqrt{\frac{\alpha(1 - \alpha) + F(1 - \alpha)^2}{\langle \hat{n} \rangle}}, \quad (5)$$

where  $F = \langle \Delta^2 \hat{n} \rangle / \langle \hat{n} \rangle$  is the Fano factor as it would be measured in the absence of the object. For a Poissonian probe,  $F = 1$ , one retrieves the SNL,  $\Delta\alpha_{\text{SNL}}$ . However, sub-Poissonian light with  $F < 1$  allows surpassing the SNL. The most favorable case is when  $\langle \Delta^2 \hat{n} \rangle = 0$  (Fock state), leading to  $\Delta\alpha_{\text{Fock}} = \sqrt{\alpha} \Delta\alpha_{\text{SNL}}$  depicted in figure 1(b), black line. Incidentally, it has been shown that the last one represents the ultimate quantum limit (UQL) in the loss estimation for a single mode interrogation of the sample [42, 45] as well as for entangled bipartite states [46]. The advantage is dramatic for small absorption, a region which is particularly significant in many real applications, for example when imaging thin biological samples or detecting low density gas flowing or low concentration in solution.

### 3.1. Twin beam

In practice, realising a single mode beam with significant sub-shot-noise fluctuation reduction is quite challenging. Another way, more effective and commonly used in experimental demonstrations, relies upon the non-classical photon number correlation among two beams, the ‘twin-beam’ (TWB) state. The idea is that one beam of the pair is used as a probe while the other acts as a reference for the quantum noise, a property that can be exploited from interferometry [73, 74] to imaging [11, 12, 75].

SPDC is one of the most efficient ways to produce quantum correlations between optical fields. This physical phenomenon was discovered at the end of the sixties [76, 77] and occurs due to the interaction between an intense optical field, usually called a pump beam, and a non-linear dielectric optical medium [78]. Basically, the phenomenon consists in the decay of one photon of the pump into two photons, named ‘signal’ and ‘idler’ for historical reasons, preserving energy and momentum (see figure 2):

$$\begin{aligned}\omega_p &= \omega_1 + \omega_2 \\ \mathbf{k}_p &= \mathbf{k}_1 + \mathbf{k}_2\end{aligned}\quad (6)$$

where  $\omega_p$  is the frequency of the pump photon and  $\omega_1$  and  $\omega_2$  are the frequencies of the signal and idler photons, respectively, and  $\mathbf{k}_j$  (with  $j = p, 1, 2$ ) are the corresponding wave vectors. Even though the emission of a pair is a quantum random process, not different from photon emission by a thermal source, the presence of one photon with a certain direction and frequency is bound to the presence of a ‘twin’ photon in a correlated spatial-frequency mode. In the high gain regime of SPDC, many photon pairs can be also generated occupying a plethora of bipartite correlated modes [12, 78]. Approximately this corresponds to the parallel generation of many entangled states, each formally written as:

$$|\text{TWB}\rangle_{1,2} = \sum_n c_n |n\rangle_1 |n\rangle_2, \quad (7)$$

where for simplicity the subscript ‘1’ represents the spatial-frequency mode  $(\mathbf{q}, \omega)$  and the subscript ‘2’ represents the correlated mode  $(-\mathbf{q}, \omega_p - \omega)$  ( $\mathbf{q}$  is the transverse momentum) [78]. The probability amplitude is  $c_n \propto \sqrt{\mu^n / (\mu + 1)^{n+1}}$ , where  $\mu$  is the mean number of photons per mode.

From the form of the coefficients  $c_n$  the super-Poissonian (thermal) character of the pair emission emerges. However, the thermal fluctuations are perfectly reproduced in the two modes. The degree of correlation is quantified by the noise reduction factor  $\sigma$ , as the ratio between the variance of the difference in the number of photons in the two modes, normalised to the corresponding shot noise [14, 79–88]:

$$\sigma = \frac{\langle \Delta^2 (\hat{n}_1 - \hat{n}_2) \rangle}{\langle \hat{n}_1 + \hat{n}_2 \rangle} \equiv \frac{\langle \Delta^2 \hat{n}_1 \rangle + \langle \Delta^2 \hat{n}_2 \rangle - 2\langle \Delta \hat{n}_1 \Delta \hat{n}_2 \rangle}{\langle \hat{n}_1 + \hat{n}_2 \rangle}. \quad (8)$$

For classical states,  $\sigma$  is lower bounded by 1, while for a TWB in the form of equation (7) it is  $\sigma_{\text{TWB}} = 0$ . Also in this case the practical limit in the noise reduction is usually represented by the unavoidable presence of losses. From equation (4), considering two modes subject to the same transmission-detection efficiency  $\eta_1 = \eta_2 = \eta$ ,

$$\sigma_{\text{det}} = \eta\sigma + 1 - \eta. \quad (9)$$

The lower bound in the presence of losses is therefore  $\sigma_{\text{det}} = 1 - \eta$ .

The sub-shot-noise (SSN) correlation of the TWB state has been experimentally demonstrated both in the case of two-mode state as in equation (7) [82, 84, 89–91] and in the case of many spatial modes detected in parallel by the pixels of a CCD camera [79, 81, 92].

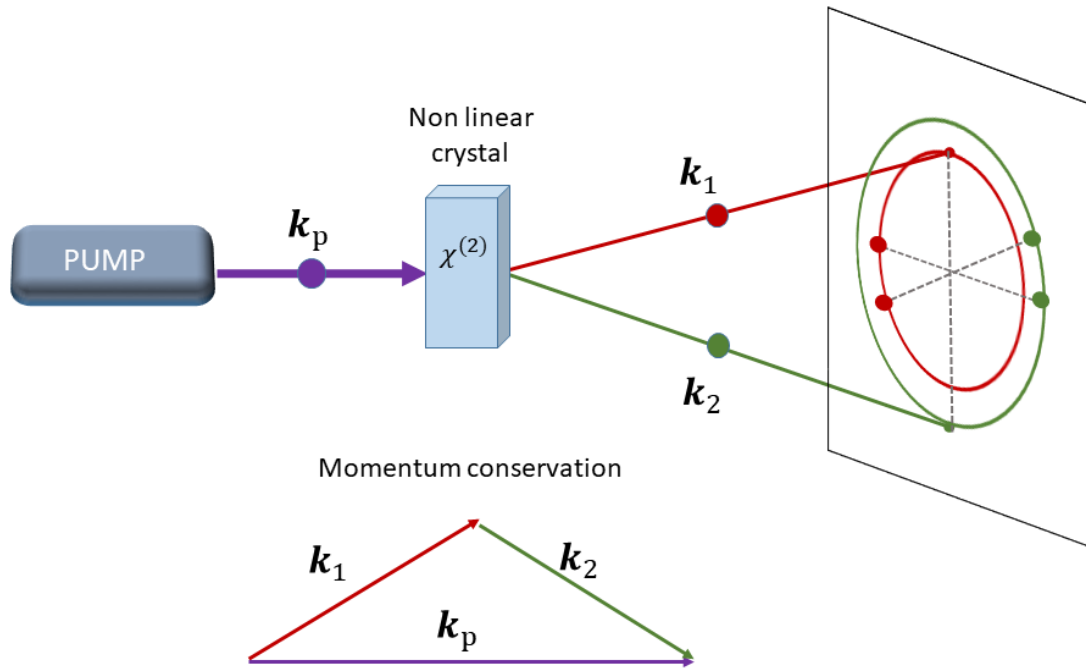


**Figure 2.** Generation of a TWB state by SPDC: the process occurs inside a crystal with second order susceptibility. A photon of an input pump field is down-converted into a pair of lower energy photons conserving also the momenta (phase matching). The phase matching condition establishes a relation between the emission angle and the wavelength (frequencies) of the photons. Thus, correlated photons appear in the opposite direction, along circles corresponding to their specific wavelength, according to the energy conservation.

SSN correlations can also be efficiently generated by four-wave-mixing (FWM) in atomic vapours [93–96], a process depicted in figure 3. A double- $\Lambda$  configuration with three atomic levels is exploited (often the hyperfine splitting structure of rubidium), so that when two pump photons are absorbed, two photons, the signal and the conjugate, are generated ( $\omega_{\text{conj}} = \omega_{\text{sign}} + 2\delta$ , where  $\delta$  is the hyperfine energy splitting). Given the intrinsic high gain of the process, and the stimulation obtained by seeding the signal with a macroscopic beam, FWM leads to the production of intense quantum correlated beams that can reach noise reduction  $\sigma < 1$  for several tens of  $\mu\text{W}$  of optical power.

Based on this strong non-classical correlation, TWB states have shown the possibility of sub-SNL sensitivity in absorption/transmission measurements [87, 97–100], quantum ellipsometry [101, 102], quantum enhanced sensing [9, 10, 103, 104], quantum reading of digital memories [105] and plasmonic sensors [106, 107]. The common idea behind these works is that the random intensity noise in the probe beam addressed to the sample can be known by measuring the correlated (reference) beam and subtracted.

These considerations can be extended to the multi-mode case. Indeed, when TWBs are produced through parametric down conversion, or by FWM in atomic vapours [96, 108, 109], the emission is spatially broadband, forming a collection of pairwise correlated modes in the transverse plane. Modern high sensitivity multi-pixel detectors, like charge coupled devices (CCDs), complementary metal-oxide semiconductor (CMOS) cameras, or single-photon detector arrays, can detect simultaneously thousands of correlated spatial modes with high efficiency, improving the sensitivity of imaging applications even in wide-field modality [6, 110–112].

One of first application of SPDC entangled photons has been ‘ghost imaging’ (GI) [113, 114], whose goal is the reconstruction of the spatial transmission/reflection profile of an object even if the interacting photons are collected by a single pixel detector. After the first realisation, it has been shown that GI can also be obtained with classical beams, nevertheless non-classical correlations provide some advantages at very low photon flux [115–117].

Finally, non-classical correlations have disclosed new possibilities in quantum radiometry [118], e.g. the possibility of absolute calibration of detectors without the need for comparison with calibrated standards. The first proposal for calibrating single-photon detectors was formulated by Klyshko [76] just after the discovery of the SPDC process and nowadays it is an established technique [13] currently used in metrological institutes. Generalising the method to the domain of analogue detectors and spatially resolving detectors has recently led to the absolute calibration of electron multiplying CCD cameras (EMCCDs) from the linear regime [14, 119] to the on-off single-photon regime [15], by just changing the intensity of the SPDC pump laser, as well as of ICCD cameras [120, 121].

### 3.2. Fock states and single-photon sources

Single-photon sources, and more generally Fock state sources, are necessary for applications in the field of quantum technologies (e.g. quantum computing, quantum key distribution and quantum metrology), which are among the most relevant topics with respect to innovation and high technology worldwide. An ideal single-photon source emits one photon on demand, at a time chosen by the user, with the emitted



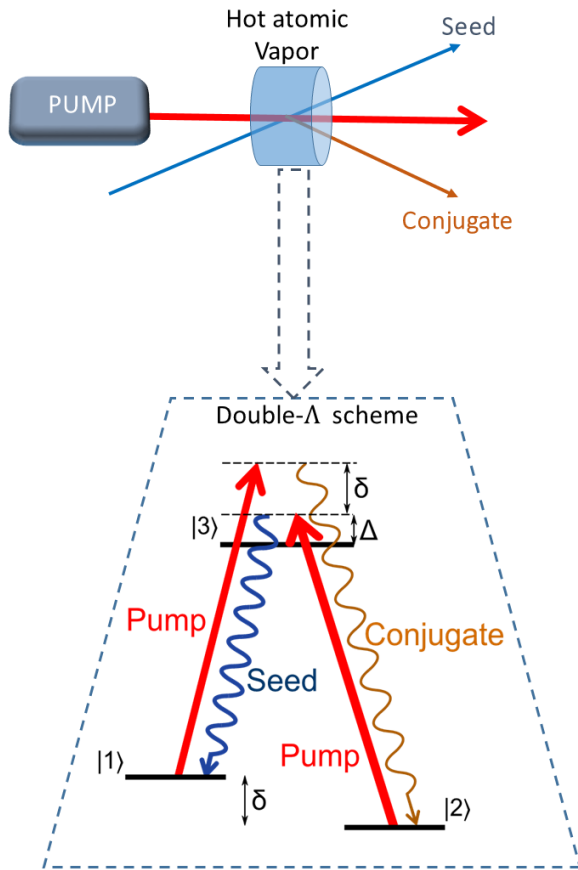


**Figure 3.** Generation of a TWB state by FWM: in this process two degenerate photons of a pump beam are absorbed in a hot atomic vapour cell operated in a double- $\Lambda$  configuration, promoting the emission of two new photons with different energies. The emission is usually stimulated by injecting a seed beam, which is amplified together with the emission of a macroscopic conjugate beam.

photons being indistinguishable from one another and having an adjustable repetition rate [122–124].

Based on these requirements, two figures of merit are generally used for characterising the quality of a single-photon source. They are represented in figure 4. The Hanbury-Brown and Twiss (HBT) interferometer in figure 4(a) measures the tendency of the photons to arrive in pairs. Formally, the HBT experiment allows the evaluation of the second order Glauber correlation function, defined as  $g^{(2)}(\tau = 0) \equiv \langle \hat{n}(\hat{n} - 1) \rangle / \langle \hat{n} \rangle^2$ . For coherent light (a stable laser) this parameter equals unity; for thermal light it turns out to be 2; while it must be zero if the photons are emitted one by one. Thus, for a single-photon source, the coincidence level between the two detectors at the varying of the temporal delay  $\tau$  presents a dip exactly at  $\tau = 0$ . The second scheme, sketched in figure 4(b) and known as the Hong–Ou–Mandel (HOM) interferometer, measures the indistinguishability of two photons produced at different times by a single-photon source. Only if the photons (or more precisely their paths) cannot be distinguished, even in principle, with respect to any degrees of freedom (polarisation, wavelength, spatial mode, etc), quantum interference happens, forcing the photons to exit always from the same side of the beam splitter and no coincidences are registered. If the two photons can be identified, for

example temporally, the interference disappears. Therefore, only for  $\tau = 0$  a dip is observed.

A Fock state source [43] is a generalisation of a single-photon source, since it should be able to emit a fixed number of photons on demand that are indistinguishable from one another. Obviously, a Fock state source emitting  $n$  photons per pulse can be realised by exploiting  $n$  ideal single-photon sources operating together. Such photon sources have the potentiality to become a new quantum standard with a huge range of applications: calibration/characterisation of single-photon counter devices [125–128], realisation of the SI base unit candela [118], quantum enhanced measurements [47], quantum sensing [103, 129] and quantum imaging.

In recent years, there has been significant progress in the field of single-photon sources and their use in metrology, also thanks to the research activities started in national metrological institutions aimed at developing metrological techniques for raising quantum technology applications exploiting single photons. In particular, single-photon sources were calibrated in a traceable way with respect to their absolute optical radiant flux and spectral power distribution [130, 131]. Although this might be considered as a huge step towards the realisation of a new photon standard source, the photon fluxes are still too low, and the purity is still insufficient for real practical use.

Indeed single-photon sources, typically, present intrinsic single-photon emission losses due to non-radiative decay mechanisms allowing the spontaneous decay of a single excited quantum emitter, without the emission of the expected single photon [23, 24]. These non-radiative mechanisms dissipate the energy associated with the quantum emitter decay in some other way, for instance in the form of phonons in solid state systems. In some cases, it is possible to effectively suppress such non-radiative decays (e.g. operating the emitter at cryogenic temperature), obtaining an almost ideal single-photon source showing nearly 100% quantum efficiency [22, 132, 133]. Even in the presence of such ideal single-photon sources, the photon flux emission is often limited by the poor optical collection and out-coupling of the emitted single photons.

To enhance the photon fluxes of single-photon sources, and make them closer to a deterministic behaviour, photonic structures for enhancing the photon collection efficiencies are required. Indeed, even exploiting high numerical aperture objectives, the collection efficiency is of the order of a few per cent. Several photonic structures for photon collection enhancement are under investigation, between them solid immersion lenses, waveguiding structures, micro-resonators or planar optical antennas [134–144].

The actual single-photon sources are still far from being completely predictable, deterministic and indistinguishable. Improvements are required to bring single-photon sources close to the ideality, but they can be already exploited in several interesting applications in the field of quantum technologies in general, and for quantum imaging applications in particular, because of their intrinsic anti-bunching or sub-shot noise properties [145].

By contrast, non-radiative and optical losses as well as decoherence limit the applicability of non-ideal sources to

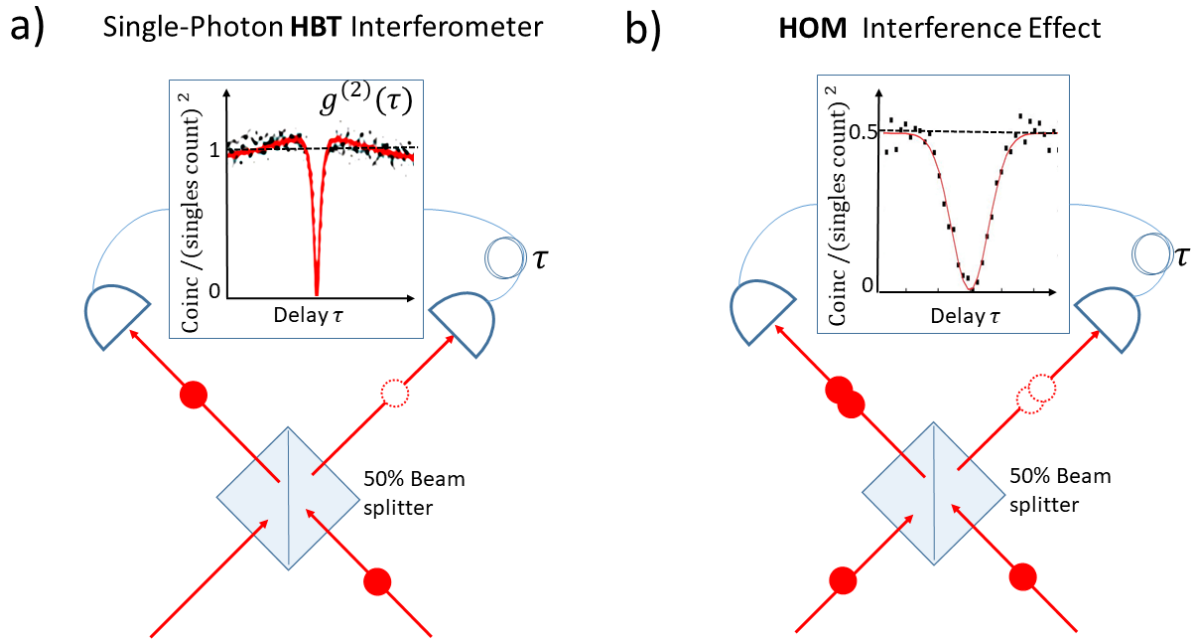


**Figure 4.** Figures of merit for characterising single-photon sources. (a) Sketch of the Hanbury-Brown and Twiss experiment. A photon impinges a 50% beam splitter: in half of the cases the photon is reflected ( $p_R = 1/2$ ) and in the other half it is transmitted ( $p_T = 1/2$ ), with no chance of having coincidences between the two detectors. If a subsequent photon arrives after a time interval  $\tau \neq 0$  there is a probability  $1/2 = p_R \cdot p_T + p_T \cdot p_R$  that the two photons are registered by different detectors. (b) Hong–Ou–Mandel effect. If two indistinguishable photons arrives at the same time ( $\tau = 0$ ) at the ports of the beam splitter, a quantum interference phenomenon occurs due to the fact that the amplitude probabilities  $\mathcal{A}_{TT}$  and  $\mathcal{A}_{RR}$  of the events of the type  $TT$  (both the photons transmitted) and  $RR$  (both the photons reflected) respectively, sum up coherently, i.e. with their quantum phases. Since each reflected photon acquires a phase  $\pi/2$ , the amplitude probability  $\mathcal{A}_{RR}$  is equal but opposite in sign to  $\mathcal{A}_{TT}$  (because  $\exp \pi/2 * \exp \pi/2 = -1$ ). Thus, the coincidence probability  $|\mathcal{A}_{TT} + \mathcal{A}_{RR}|^2$  is null.

scenarios where deterministic emissions of ideal and completely identical single photons are necessary, such as, e.g. when interference/interaction between two (or more) single photons is exploited, as in quantum computation or simulation. Moreover, from the metrological point of view, ideal single-photon sources on demand are highly desirable for developing absolute sources with finite photon number emission without intensity fluctuation. This could lead to a redefinition of radiometric and photometric units in terms of the number of photons (quantum Candela) [118].

We highlight that a reasonable approximation of single-photon sources are the heralded photons produced by SPDC [146, 147]. As mentioned in section 3.1, photons are always emitted in pairs with low probability, but one can get rid of the vacuum component since the detection of one photon of the pair heralds the presence of the other one, and the probability of double pair emission remains very low. These pseudo single-photon sources, based on SPDC or FWM, have interesting performances in terms of photon rate [124] and quality of the single-photon emission, but they typically need temporal post-selection [124] to distinguish the heralded photon from a dominant unheralded background photon (even if there are remarkable exceptions [146, 148]).

Despite the fact that temporal post-selection is a limiting factor for the possibilities of practical exploitation of heralded single-photon sources in quantum technologies, this approach has been demonstrated recently for quantum enhanced absorption measurement and spectroscopy of a biological sample (haemoglobin) with post-selection of the heralded single

photons [149], and with selection performed by active feed-forward enabled by an optical shutter [150].

When it is possible to exploit temporal post-selection, e.g. for pulsed TWB emission, we should note that TWB, multi-modes or in the high gain regime, can be exploited as an heralded Fock state source, having on the heralding arm a photon number resolving detector with (nearly) ideal unit efficiency.

## 4. Quantum imaging

Quantum imaging is one of the first application of quantum photonic technology [75], where the quantum properties of light are exploited to enhance some peculiar aspect of the image formation process.

### 4.1. Super-resolution with single-photon emitters

Fluorophores and markers used in biological microscopy can be chosen among single-photon emitters such as quantum dots, dye molecules or NV centres in (nano)diamond. A single-photon emitter presents, by definition, a strong anti-correlation in the temporal photon emission, since at any time the presence of more than one photon is prevented by the excitation-decay process (see figure 4 and its discussion in the text).

This effect is known as anti-bunching and can be exploited in many applications, from quantum information and communication to metrology and super-resolution imaging.

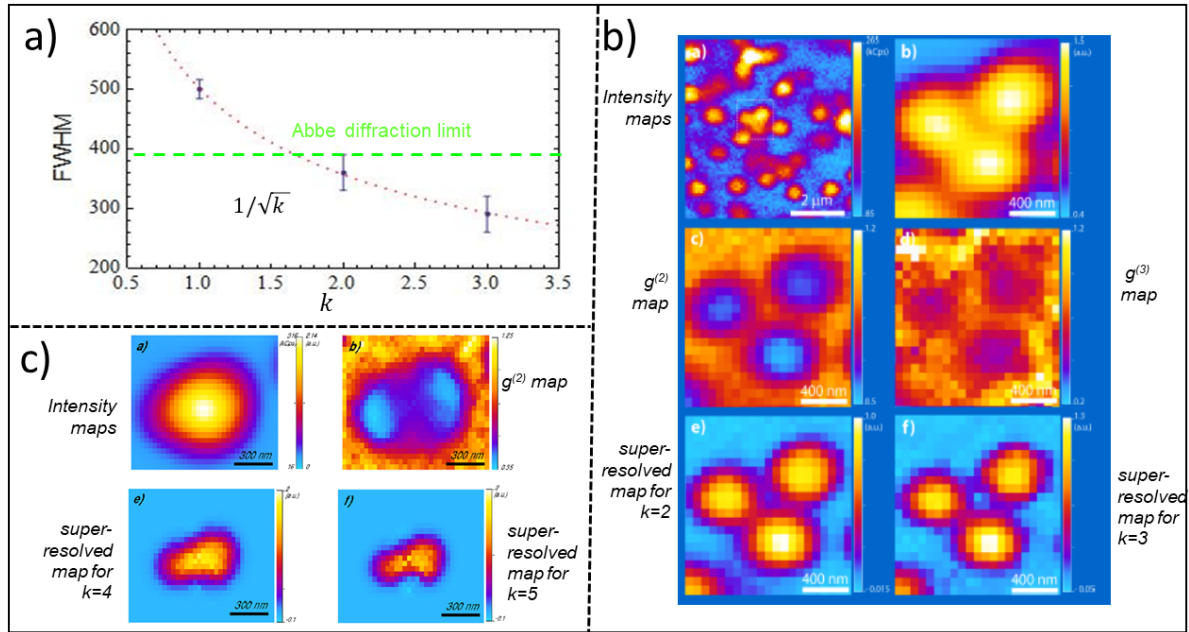


**Figure 5.** Super-resolution by exploiting anti-bunching in a confocal single-photon microscope [153]. (a) Experimental scaling of the FWHM of the point spread function with the order of the coincidence  $k$ . The green dashed line is the theoretical DL. (b) From the top to the bottom: intensity map showing three NV centres close to the DL separability, two- and three- fold coincidences maps, super-resolved map using the extra information gained by the measurement of  $g^{(2)}$  and  $g^{(3)}$ . The white bar is 400 nm long. (c) Two emitters are at a distance below the DL and cannot be distinguished by looking at the intensity map. From the  $g^{(2)}$  function (two-fold coincidence of photons) the presence of two dips suggests the existence of two distinct centres and this information is used in the super-resolved images (it is safely assumed that  $g^{(k>2)} = 0$ ). The black bar is 300 nm long.

A possible approach exploits the measurement of the higher order Glauber correlation function at  $\tau = 0$ ,

$$g^{(k)}(\tau = 0) = \frac{\langle \prod_{i=0}^{k-1} (\hat{n} - i) \rangle}{\langle \hat{n} \rangle^k}, \quad (10)$$

in each position of the image plane, obtaining an increase in the resolution of the single-photon emitters map. Indeed if two or more single-photon emitters are closer than the DL, thus indistinguishable from the standard fluorescence intensity map, the presence of coincident single-photon detection indicates the presence of more than one single-photon emitter. This additional information, together with the intensity map, allows the reconstruction of a super-resolved map [151–153]. In general, for an arbitrary number of centres in the cluster, a resolution improvement factor of  $1/\sqrt{k}$  is achieved when the Glauber autocorrelation function is measured up to the  $k$ th order ( $g^{(k)}$ ).

Experimental demonstrations of this technique have been performed in wide-field and in confocal microscopy [152, 153]. Figure 5 presents some of the results obtained in [153], by exploiting NV centres in a single-photon confocal microscope.

Recently it has been proposed to combine this high order correlation function method with the use of structured excitation light [154]. It has been shown that in this case one could reach a resolution increase of  $k + \sqrt{k}$  with respect to the DL.

Another technique, realised in 2017 [155], exploits anti-bunching together with the natural ‘photoblinking’ effect found in many types of fluorophores and a fibre bundle collecting light with certain spatial resolution. After the reconstruction, a final resolution of 20 nm was reported.

It is worth mentioning the research on sub-diffraction imaging triggered by the interesting paper by Tsang and coworkers [156]. In their quantum-estimation-inspired proposal [157], they observe that, given only two single-photon emitters, a lot of information is present in the sum of the electromagnetic field of the two emitters at the image plane rather than just the sum of the intensity alone. Thanks to this, and using the quantum estimation theory, they were able to devise imaging techniques able to beat by far the diffraction limit. The idea of identifying the ultimate bound of the ability to estimate the distance between a pair of closely separated sources, achieving near-quantum-limited performance has inspired a relevant amount of theoretical researches (see e.g. [158–161]), and also a certain amount of proof-of-principle experiments (see e.g. [162–166]). It is important to notice that all these results are limited to the case of only two sources; it is far from being obvious that similar performance can be achieved in the case of three or more sources. It is expected that this becomes an active research field in the future years also because of its inherent connection with the multi-parameter quantum estimation problem [157, 167].

#### 4.2. Sub-shot-noise imaging

Extracting relevant information about a delicate sample with the lowest photon dose is of paramount importance in biochemistry and biology to ensure that the processes being investigated are not shifted to an alternate pathway due to environmental stress. Wide field microscopy is the simplest, fastest, least expensive and oldest imaging solution used, for example, for live-cell imaging and it has the advantage of

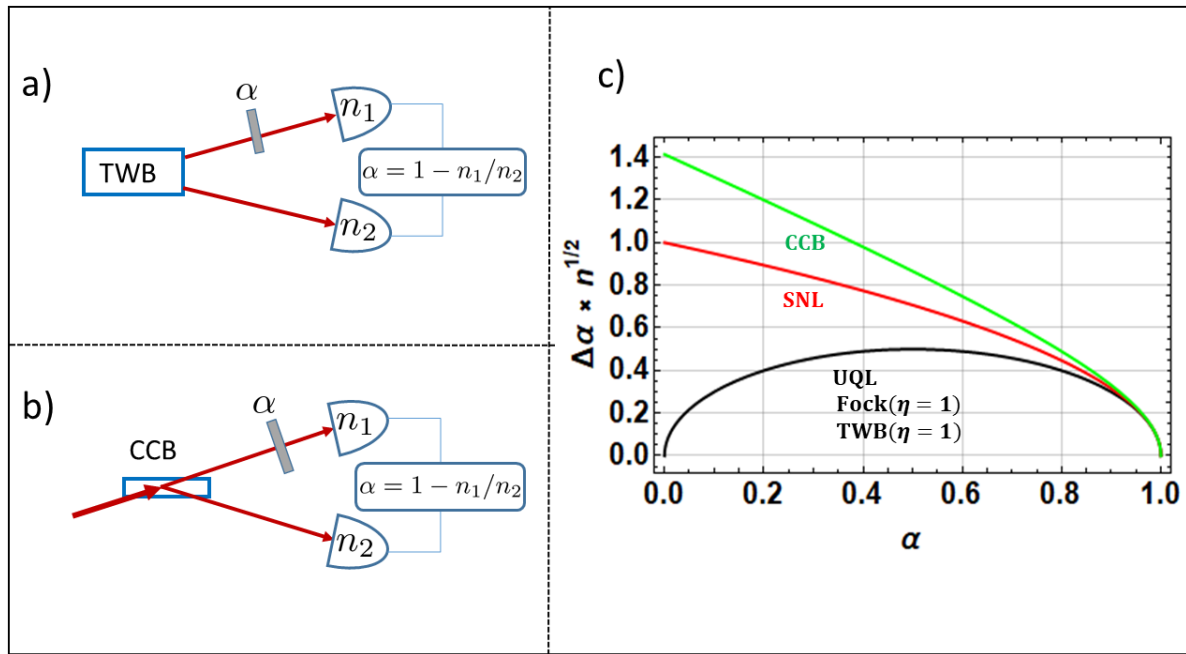


**Figure 6.** Loss estimation with correlated beams. (a) A pair of quantum correlated beams, i.e. a twin-beam (TWB), is used: one beam is the probe interacting with the sample, while the other beam is the reference. (b) Classically correlated beams (CCB), e.g. obtained by splitting a thermal beam, are exploited. (c) Uncertainty in function of the loss parameter  $\alpha$  for the TWB (ideal detection efficiency  $\eta = 1$ ) and the CCB cases compared to the shot noise limit (SNL) and to the ultimate quantum limit (UQL).

requiring the lowest photon dose, especially in transmission imaging with respect to scanning confocal microscope [168].

The exploitation of multi-mode correlations in a TWB has been proposed for high sensitivity wide field imaging of a weak absorbing object in [110] and a proof of principle of this technique has been reported by Brida *et al* in 2010 [111]. Recently, the first wide-field sub-SNL microscope [6] was realised, providing images of  $10^4$  pixels with a true (without post-selection) significant quantum enhancement, and a spatial resolution of few micrometres. This represents a considerable advancement towards a real application of quantum imaging. In the following we will discuss some details of this application.

We have already seen that sub-Poissonian light can be used to achieve SSN absorption estimation according to equation (5). However it is challenging to experimentally produce single modes with sub-Poissonian photon statistics. A different approach is to consider two correlated modes from a TWB state, and using one of them as a reference for the noise in a ‘differential’ scheme, as presented in figure 6(a). In this case the uncertainty is:

$$\Delta\alpha_{\text{TWB}} \simeq \sqrt{\frac{\alpha(1-\alpha) + 2\sigma_{\text{det}}(1-\alpha)^2}{\langle N_P \rangle}}, \quad (11)$$

where  $\sigma_{\text{det}}$  is the the noise reduction parameter in equation (9). For a TWB it equals the losses in detecting correlated photons,  $\sigma_{\text{det}} = 1 - \eta$ . Ideal lossless detection leads to the ultimate quantum limit,  $\Delta\alpha_{\text{TWB}} = \sqrt{\alpha}\Delta\alpha_{\text{SNL}} \equiv \Delta\alpha_{\text{UQL}}$ , which is represented by the black curve in figure 1(c). The performance of a TWB in loss estimation has been theoretically discussed in [97–100] and demonstrated experimentally in [87, 99, 100]. In [100] more than 50% sensitivity improvement

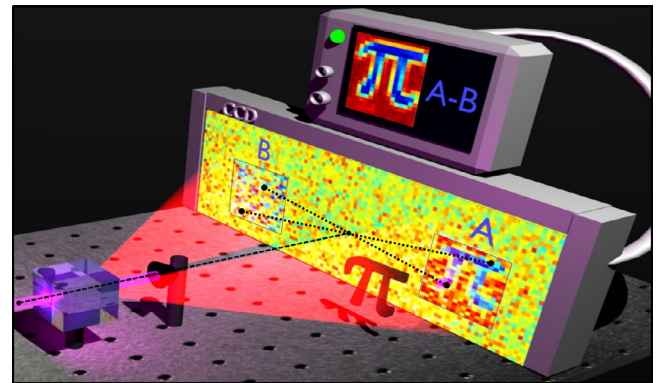


**Figure 7.** Simplified representation of a sub-shot-noise imaging scheme. The quantum noise in the probe beam, where a faint absorbing object is placed, can be removed by subtracting from the signal measured in each pixel of the image the noise measured in the corresponding symmetric pixel in the correlated beam.

with respect to the SNL was reported, and it reached a 100% improvement when compared with conventional two-beam approach, represented in figure 6(b). Note that the two-beam approach is extensively used in standard devices like spectrophotometers, where a classical beam is split in two and one beam is used to monitor the instability of the source and detectors and to compensate for them. However, in classical correlated beams (CCBs) generated in this way, only the super-Poissonian component of the fluctuations is correlated (sometimes called classical ‘excess noise’), whereas the shot noise remains uncorrelated and cannot be compensated. Indeed the TWB represents the natural extension of this method to the quantum regime. Recently similar schemes, but exploiting four wave mixing in rubidium vapour, have been applied for



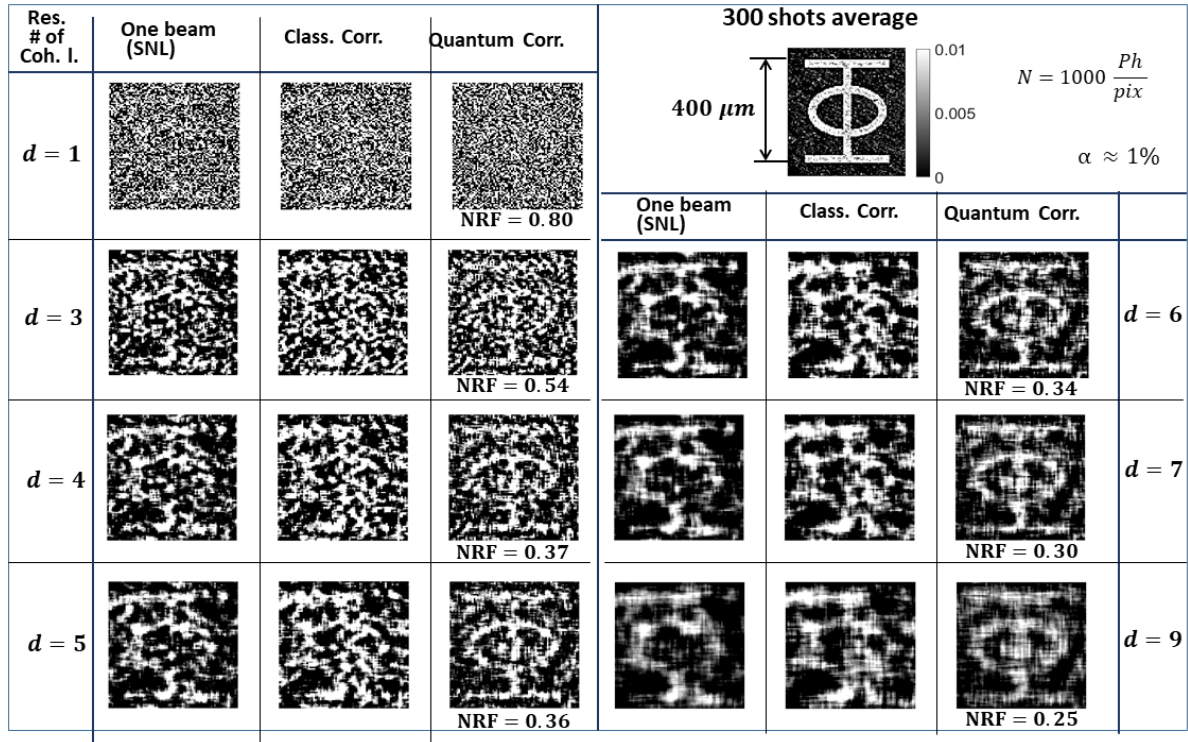


**Figure 8.** Experimental single-shot images extracted from [6]. Direct classical imaging, imaging exploiting classical correlation and imaging exploiting quantum correlation are compared.  $d$  is the spatial resolution parameter, such that the effective resolution is  $d * L_{coh}$ , where  $L_{coh} = 5 \mu\text{m}$  is the spatial coherence length of the TWB correlation at the object plane. The mean number of photons detected per pixel per frame is  $N \sim 1000$ . The upper-right panel is the object image averaged over 300 shots.

monitoring index refraction change in plasmonic sensors [106, 107].

The extension of the technique from the two-mode case to the multi-mode case allows the realisation of wide field SSN imaging, as represented schematically in figure 7. Basically, it is possible to match the pixel structure of a spatially resolving detector with the spatial distribution of the multi-mode TWB generated in the SPDC process, so that each pair of correlated spatial modes is precisely and entirely detected by a pair of pixels. The quantum correlation in transverse momentum, between  $\mathbf{q}$  and  $-\mathbf{q}$ , is converted in spatial correlation among symmetric pixels in position  $\mathbf{x}$  and  $-\mathbf{x}$  at the object plane by a far-field lens (not shown in the figure). The noise of the image taken in one branch is removed pixel-by-pixel by ‘subtracting’ the noise pattern measured on the other branch [111]. In [6], the method has been demonstrated in a microscope configuration, using a CCD camera operating in linear regime, with high quantum efficiency (95%) and low noise (few electrons per pixel per frame). The experimental evidence of the noise reduction and the sensitivity improvement obtained is presented in figure 8.

The spatial resolution of this technique is given by the traverse size of the correlation (coherence area), namely the uncertainty in the relative propagation direction of correlated photons, which is proportional to the inverse of the pump width. Pixel size should be large enough to include at least a coherence area, otherwise correlated photons may be lost affecting the noise reduction factor. In fact, figure 8 shows that at full resolution ( $d = 1$ ) the noise reduction is modest while it becomes better if the resolution decreases.

Finally, we mention that several proofs of principle of quantum enhanced phase-contrast scanning microscopy exploiting NOON states ( $N = 2$ ) [62–65] have been reported, although, in most of the cases, a significant enhancement without post-selection or losses compensation is still missing.

#### 4.3. Quantum enhanced displacement sensing

Sub-shot-noise photon number/intensity correlations enable detection of the displacement of a light beam with accuracy surpassing standard methods based on laser beams. The standard way to monitor the wandering of a light beam is to send it to a quadrant detector as depicted in figure 9(a). This configuration is used for measuring small displacements in many applications, for example, in atomic force microscopy, ultra-weak absorption measurements, or single molecule tracking in biology [5, 71]. When the beam is perfectly aligned to be symmetric with respect to the origin of the axis, the difference in the power measured in the different sectors is, on average, null. Small displacement in one direction, for instance along the  $x$ -axis, will give a proportional change in the photocurrent difference [169],

$$\langle n_{A+C} - n_{B+D} \rangle = \frac{2}{\pi^{1/2}} \frac{\delta x}{w} N, \quad (12)$$

where  $w$  is the waist of the beam (let us suppose a gaussian beam) and  $N = n_{A+C} + n_{B+D}$  is the total photon number in the beam. However, due to the shot noise, which is independent between right and left sectors, the noise on the right side



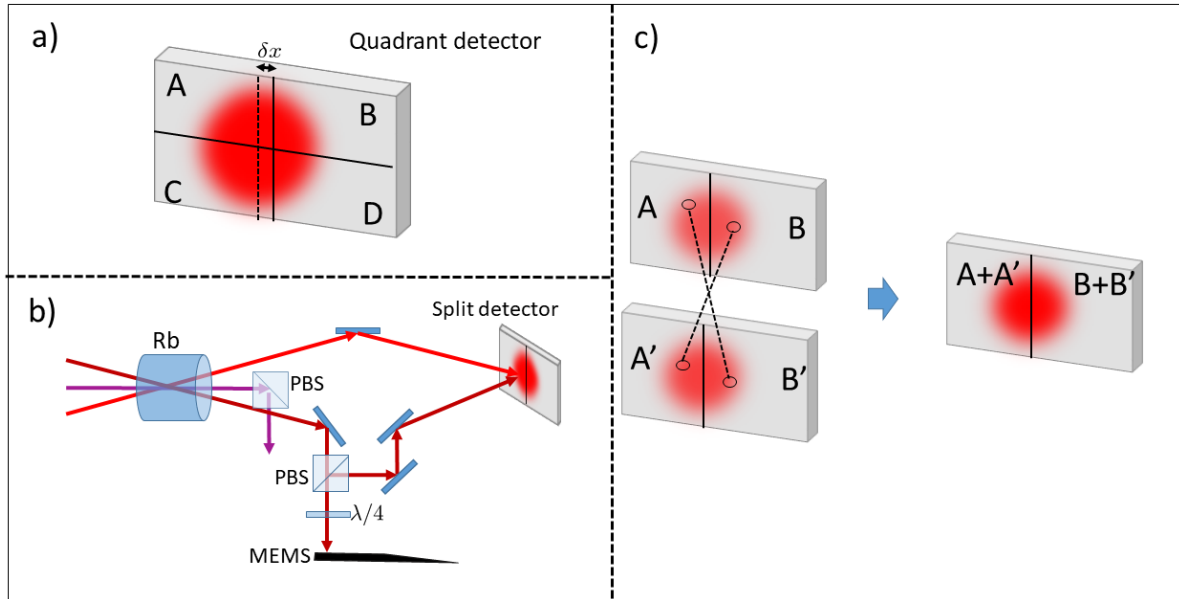


**Figure 9.** Beam displacement measurement. (a) Quadrant detector configuration. (b) Differential beam position measurement with a quantum correlated TWB from four-wave mixing in rubidium (Rb). The probe is sent to a polarising beam splitter (PBS), then it passes through a quarter-wave plate before being focused onto a micro cantilever (MEMS). On the return path the probe beam is separated at the PBS and sent to a split detector and overlapped to the reference one. (c) Scheme of the spatial correlations at the split detector.

of equation (12) is exactly  $N^{1/2}$  and the minimum detectable displacement becomes:

$$\Delta x = \left( \frac{\pi^{1/2} w}{2} \right) \frac{1}{\sqrt{N}}. \quad (13)$$

It is interesting to note that the spatial resolution limit in this case is given by the energy available in the beam, or the power limit supported by the quadrant detector.

Multi-mode quantum correlations allow beating the SNL in equation (13). Following previous theoretical investigation [170], the first demonstration of SSN displacement detection along one dimension was obtained in [171] by combining vacuum squeezed beam and a coherent beam that were spatially orthogonal. Although the resultant beam is not squeezed globally, it is shown to have strong (non-classical) internal spatial correlations between the portions of the beam impinging different sectors of the detector. The technique has been extended in the 2D case in [72].

An evolution of this technique has led to the experimental demonstration of sub-shot-noise particle tracking in living systems and microrheology within *Saccharomyces cerevisiae* yeast cells [71]. Lipid granules were tracked in real time as they diffused through the cytoplasm surpassing the SNL of 42%. In typical laser-based particle tracking, the presence of a particle causes light to be scattered out of an incident field. The interference between scattered and transmitted fields leads to a deflection of the incident field proportional to the displacement of the particle. The difficulties of using quantum correlation in this context are that, on one side such measurements are typically conducted at low frequencies where technical noise is dominant with respect to the shot noise, and on the other side, the distortion of the spatial mode propagating through high-numerical optical system and biological samples prevents the quantum light from matching the detection mode

(quadrant detector). To circumvent these issues, in [71] two separate fields are used, one for interrogation and the other a ‘flipped’ Gaussian local oscillator to define the ‘detection mode’. Interference among them, measured by a single photodiode, provides particle information equivalent to a quadrant photodiode.

In 2015, Pooser *et al* demonstrated a noise reduction of 60% below the SNL in state-of-the-art displacement sensitivity for a MEMS cantilever [9]. They used a quantum beam of power up to hundreds of  $\mu\text{W}$  reaching a few  $\text{fm Hz}^{-1/2}$  resolution in the region of  $10^5$  kHz. Figure 9(b) presents the sketch of the experiment where two spatially multi-mode correlated TWBs, generated by FWM, are superimposed at a split detector. As we discussed in section 4.3, the variance of the photocurrent difference between symmetric portions of the two beams in figure 9(c), either A and B’ or A’ and B, is lower than the SNL. Moreover, this is true also when they are spatially overlapped at the same detector. Therefore the fluctuations of the left side of equation (12) are reduced below the SNL and this is the origin of the advantage of the technique.

We mention also that a similar scheme has been investigated in the discrete case, considering spatially entangled biphoton pairs [172]. In principle, it has been found that the smallest resolvable parameter of a simple split detector scales as the inverse of the number of pairs (Heisenberg scaling) when this number is very small.

In a different perspective, but conceptually analogous to the previous case, there is the estimation of the displacement of a shadow casts by a fully opaque object intercepting a probe beam. In [173], a noise reduction corresponding to an improvement in position sensitivity of up to 17% was obtained with bi-photon pairs, created with SPDC and detected by an EMCCD camera employed as a photon-number-resolving split detector. As reported in the literature [15], the EMCCD

can be operated as a photon number resolving detector, thanks to spatial multiplexing, where each pixel is operated in the ‘on–off’ regime by setting a discriminating threshold.

#### 4.4. Quantum ghost imaging and spectroscopy

Quantum ghost imaging (QGI) and ghost-spectroscopy (QGS) are two complementary techniques based on signal and idler photons correlations in SPDC (or FWM).

QGI was proposed in 1994 [113] and experimentally realised in 1995 by Pittman *et al* [114]. It makes the reconstruction of the transmittance (or reflectance) profile of an object, placed in the signal beam, possible, although the light after the interaction is collected by a single pixel or ‘bucket’ detector, i.e. without spatial resolution. The spatial information is retrieved by performing correlation measurements (e.g. temporal coincidence) among the single pixel detector and each pixel (or position) of a spatially resolving (or scanning) detector on the idler beam. The working principle is the following: the spatial selection performed in the idler beam automatically identifies a small range of allowed positions for the correlated signal photons at the object plane, expressed by a function  $\Gamma(x_i + x_s)$  peaked into zero and which has to be narrower than the minimum size of the object variation scale. If a coincidence is registered between the two detectors, this means that in the spatial resolution cell identified in that way, the object is transmitting. On the other hand, if the coincidence is missed, the object has absorbed the signal photon. In this way, by measuring the number of coincidences  $R(x_i)$  in function of the position  $x_i$  of the idler pixel, it is possible to reconstruct the whole transmission  $T_s$  of the object in the signal path,  $R(x_i) \propto \int_{\text{Bucket}} \Gamma(x_i + x_s) T_s(x_s) dx_s \simeq T_s(-x_i)$ . Instead of measuring time coincidences between SPADs operated in on–off modality, it is also possible to measure temporal correlation of the intensity fluctuations between a couple of linear detectors if they are sensitive enough to register such signals, which are usually faint.

A lively debate as to whether ghost imaging truly requires quantum light started just after its first demonstration. Many theoretical investigations [174–176] and experiments [177–181] have demonstrated that almost all the quantum ghost imaging features can be mimicked by classical correlation, usually generated by splitting a spatially incoherent single pseudo-thermal beam (see figure 10) obtained from a laser beam scattered by a rotating ground-glass disk (not shown in figure). However, thermal GI can be obtained with sunlight [182] or a broadband super-luminescent diode source [183] although the short coherence time make the detection scheme rather difficult. An interesting compromise between thermal-light-based and TWB-based GI can be found in [184], where the authors use speckle correlation in an intense TWB seeded with thermal light.

Even computational techniques allow GI reconstruction [185–187], by impressing random spatial patterns on a single beam modulated in a controllable and known way (spatial light modulators, either in phase or amplitude are standard devices currently used in many imaging applications).

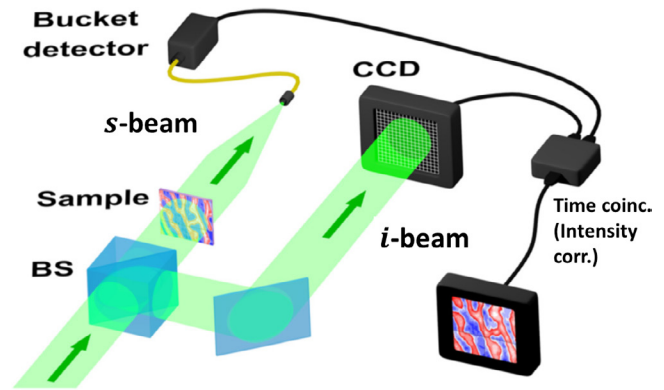


**Figure 10.** Sketch of a typical thermal ghost imaging set-up: a single beam with thermal fluctuation in space and time is divided by a BS. The signal and idler branches are imperfect copies of the same beam and therefore they share some degree of correlation. Due to the brightness of the thermal sources, correlation among the intensity fluctuation of the photocurrents are usually evaluated for the reconstruction, instead of the coincidences. (See the original picture in [204].)

Since the first proof-of-principle demonstrations, either with TWBs or with classical light, substantial advancements towards the applicability of GI have been achieved: drastically improving the SNR by differential GI [188], measuring reflected photons [189], using polychromatic light [190, 191], and extending GI to 3D reconstruction [192]. For enhancing visibility and contrast of GI, the use of high-order correlations has been proposed and applied [180, 193, 194]. Also compressive sensing techniques have been successfully transferred to GI, speeding up the image reconstruction [187, 195].

There is a really huge amount of literature on GI, both concerning its relation with more fundamental questions about the quantum-classical boundary and applications. We do not intend here to be exhaustive and we advise the interested reader to refer to dedicated reviews [176, 196].

Among the general advantages of ghost imaging that have intrigued scientists there is robustness against effects like scattering and phase distortion that are experienced between the object and the bucket detector. This can have important applications in an open-air ranging system or for inspecting biological samples, where tissues represent the diffusive medium. In fact, even if the propagation directions of photons are scrambled after the sample, it does not make any difference to the bucket detector, which integrated in any case. Many works have demonstrated turbulence free ghost imaging and ghost imaging through turbid media [188, 197–199].

Another possibility offered by QGI that is difficult to emulate with classical sources is ‘two-colour’ GI [200–202]. By producing pairs of non-degenerate photons, the object can be illuminated by photons with a significantly different wavelength from the ones detected with spatial resolution on the second beam. For example, image reconstruction in the infrared range can be achieved with cameras operated in the visible spectrum [203]. Moreover, GI is always an option in all the situations in which space constraints or ‘hostile’ environment conditions, such as e.g. extreme temperature or high electromagnetic fields, do not allow to set-up an imaging system with

a spatially resolving detector close to the sample. As proof of principle, in [204] the authors apply the GI approach to image the magnetic domain structure of an yttrium iron garnet sample by exploiting the Faraday effect, opening up possible development of magneto-optical imaging at extreme cryogenic temperatures or in the presence of high magnetic fields.

In conclusion, one of the big advantages in using quantum correlation is given by the ability of rejecting external technical noise and, in general, uncorrelated background, especially when faint light levels are required [7, 116, 117]. Furthermore, note that the noise can also be due to uncorrelated photons produced by the same source used for GI. Indeed, all the spatio-temporal modes collected by the bucket detector that are not correlated with the spatial-mode impinging on a specific pixel of the spatially resolving detector contribute to the uncorrelated background.

Basically, since the photons are produced in pairs at the same time the coincidences among two SPADs appear within a very short time window  $\Delta t$  (typically a few ns, because of the detectors and correlation/coincidence-electronic jitter). The number of ‘true’ detection events seen by each detector is simply given by  $N_{i(s)}^{(T)} = \eta_{i(s)} P \Delta t$ , where  $P$  is the pairs production rate. Analogously, the background counts are  $N_{i(s)}^{(B)} = B_{i(s)} \Delta t$  with  $B_{i(s)}$  the rate of background counts. The number of true coincidences is proportional to the probability of joint detection by the two single-photon detectors (located in the two channels)  $R^{(T)} = \eta_i \eta_s P \Delta t$ . Assuming that noise photocounts of the two single-photon detectors are uncorrelated, the number of accidental coincidences  $R^{(A)}$  is given by the product of the probability components due to accidental overlap of SPDC and noise photocounts,  $R^{(A)} = N_i^{(B)} N_s^{(B)} + N_i^{(B)} N_s^{(T)} + N_i^{(T)} N_s^{(B)} = [B_i B_s + (\eta_i B_i + \eta_s B_s) P] (\Delta t)^2$ , where we observe that it scales as the square of the detection time window. Let us suppose that the background rate is dominant, i.e.  $N_{i(s)}^{(B)} \gg N_{i(s)}^{(T)}$ . The signal to noise ratio of quantities proportional to the true coincidence is  $\text{SNR}_{\text{QGI}} = R^{(T)} / R^{(A)} \simeq \eta_i \eta_s P / (B_i B_s \Delta t)$ . This performance should be compared with the direct single branch case in which the SNR is  $\text{SNR}_D = N_s^{(T)} / N_s^{(B)} \simeq \eta_s P / B_s$ . Therefore, the advantage in terms of SNR of the quantum correlation technique is  $\text{SNR}_Q / \text{SNR}_D = \eta_i / (B_s \Delta t)$  [205]. *This means that QGI delivers better image quality reconstruction when the efficiency of the reference (idler) arm is high and the number of photons in the detection time is smaller than unity.* This also remains valid in the case of analogue detection, in which, rather than temporal coincidence, intensity correlations are measured, as derived theoretically and demonstrated experimentally in [117]. In [7], QGI of a wasp wing was obtained by less than 0.5 photon detected per pixel, with the help of a dedicated compressive sensing algorithm. In that case an intensified CCD camera was gated by the photons arriving at a SPAD, which played the role of the single pixel detector. An imaging preserving delay line is necessary to compensate for the time necessary for the electronics to send the triggering input to the camera.

Similar to ghost imaging, in quantum QGS, the correlation in frequency shown in equation (6) allows the retrieval of the absorption spectrum of  $T_s(\omega_s)$  by measuring the temporal coincidences among photon pairs  $R(\omega_i) \propto T_s(\omega_p - \omega_i)$ , and the spectral selection can be done in the beam that does not interact with the object. The first proposals and experiments have been reported in [206] and [207]. This scheme provides the same advantages of ghost imaging, offering the possibility of spectral selection in range significantly different with respect to the one of the light impinging the sample [208]. The second benefit is that the spectral profile can be obtained by exploiting an extremely low signal level compared to external and technical noise [205]. Again, it is very promising in all those applications in which delicate or photosensitive systems require the lowest dose of photons, such as in biological spectroscopy. We mention that even ghost spectroscopy can be realised with classical light, but in a completely different regime [209].

#### 4.5. Other advanced quantum imaging protocols

**4.5.1. Imaging and spectroscopy without photon detection.** We have seen that QGI and QGS allow one to measure the spatial and spectral properties of a system without spatial and spectral selection of the photons interacting with it. More complicated schemes, which use the non-linear interference occurring in non-linear crystals, allow even to eliminate the necessity of detecting those photons at all [8]. A non-linear interferometer is equivalent to a Mach–Zehnder one, where the two beam splitters are replaced by two non-linear crystals [210]. The signal and idler beams are produced in the first crystal from the pump beam. The peculiar feature of non-linear interference is that it involves a precise phase relation between all three propagating photons, i.e. the signal, the idler and the pump. Only if they have the right phase relation an output from the second crystal is observed. This differs from conventional interferometry, where the interference pattern is defined by the phase of the signal photon. Measuring the output intensity of the idler beam after the second crystal allows one to infer the phase eventually acquired by the signal beam passing through a sample. Here, the detection of signal photons is not necessary. Similar processes can open up entire new metrology schemes in optical imaging and sensing. Non-linear interference has been used in imaging protocols with undetected photons [211], interferometry below the shot noise [212, 213] and hybrid atom–light interferometers [214].

**4.5.2. Quantum illumination.** Quantum illumination (QI) is a protocol proposed in 2008 by Lloyd [215] and soon reformulated exploiting a TWB by Shapiro *et al.*, [216, 217], providing a quantum improvement in target detection (radar-like configuration) in the presence of a dominant thermal background. A probe beam is addressed to a region of space where a weak reflecting target may be present or not. However, the partial reflection of the probe beam is hidden in a much stronger background. A quantum receiver performing a joint measurement between the reflected probe and an ancillary quantum correlated beam allows the discrimination of the



faint signal component from the noise, revealing the presence of the target. Indeed QI with TWB delivers a 6 dB (a factor of four) improvement in the error probability exponent with respect to the best classical strategy.

The outstanding feature of quantum illumination, which makes it unique in the panorama of quantum enhanced measurements, is that its advantage does not depend on either losses or on the noise the probe experiences during the propagation and the interaction with the target. It is important to note that both these processes cause decoherence and therefore the initial entanglement or quantum correlation, is completely lost at the detection stage. This property is very valuable, especially in view of real world applications, where noise and losses are often unavoidable.

A first experimental realisation of a quantum illumination-like protocol was reported in [103, 218] considering a restricted scenario in which only intensity measurements (phase-insensitive) were exploited. Here a photon number measurement was performed independently in the reference arm and in the probe arm, then the covariance of the two quantities was evaluated. In this case, because of the high correlation in the TWB, unreachable by classical beams, the quantum advantage scales as  $1 + M/n = 1 + 1/\mu$ , where  $M$  is the number of spatio-temporal modes (the inverse of the bandwidth) and  $\mu$  is the mean number of photons in each mode. Interestingly, this corresponds to increasing the total mutual information between two parties sharing a quantum correlated states with respect to the one provided by classical correlations [219]. In [103, 218] a 10 dB improvement in terms of SNR with respect to correlated thermal beams was achieved.

A quantum receiver able to beat the performance of the optimal classical strategy by 3 dB was realised in [10], based on an optical parametric amplifier scheme [216, 220]. The advantage, however, requires that the returning probe, when present, has known amplitude and phase, which is not the case in many light detection and ranging (lidar) applications. At lidar wavelengths, most target surfaces are sufficiently optically rough that their returns are randomly distributed in amplitude and phase (speckles). In [221] the authors show that second harmonic generation process allows enhancing the detection of Rayleigh-fading targets, although with reduced (subexponential) advantage. The same receiver, in the case of a non-fading target, achieves QI's full 6 dB advantage [222]. Further improvements can be, in principle, obtained by using photon-subtracted two-mode-squeezed states [223], although their practical realisation is extremely challenging.

Recently microwave/optical QI was proposed in [224]. It would be of utmost importance to move from the optical demonstration to the microwave region because it is the natural domain in which QI could have vast application in the field of remote sensing. Quantum illumination has potential application also in the field of secure quantum communication, for defeating passive eavesdropping attacks [225, 226]. The idea is that only authorised parties that share the original quantum correlations can achieve information on the modulation of an weak reflection, if enough noise is artificially added in the channel.

Quantum illumination can also find application in biological measurements when a delicate probing is essential and, at the same time, the surrounding environment background can be of disturbance.

## 5. Quantum photometry

One of the strongest motivations for developing single- and few-photon metrology is related to the investigation of the response of biological systems at the few-photon level. Some biophysical and biochemical processes, for example photo-transduction in vision, or photosynthesis, are triggered by the absorption of a single or few photons. The physical stimulus of vision is a consequence of the interaction between single photons and a family of light-sensitive proteins called opsins, typically found in photoreceptor cells present in the eye. Our visual system provides hundreds of millions of photoreceptors, divided into two families of photosensitive cells, rods and cones, that allow eye sensitivity to a huge range of luminance values (ranging from  $105 \text{ cd m}^{-2}$  down to the single-photon level). This system converts the light pattern in an electrical pattern, later processed and sent to the optical nerve by other cells present in the retina (ganglion and interneurons). Under high illumination levels, rods saturate and only cones, divided into three classes according to different spectral sensitivity, contribute to the vision (photopic vision). As the level of light decreases, rods start to be active (mesopic vision) together with cones, below a certain luminance level ( $10^{-2} \text{ cd m}^{-2}$ ), only rods are operative (scotopic vision) [118].

Rods are recognised as acting as photouncounters with very high quantum efficiency and low dark noise [227]: evidence of the detection of few photons is present in literature since 1942 [228]. In this pioneering work, a Poissonian source of photons was considered and compared to the statistics of the response of a dark-adapted human observer, demonstrating that such an observer is able to detect very few photons (5–7 photons). However, the response of the retina at the single- or few-photon level is not easy to be investigate with classical light sources, dominated by shot noise for low photon fluxes causing random multiphoton events. As discussed in this paper, only quantum optical sources of light allow this limitation to be overcome. The development of deterministic single-photon sources, based on time correlated photon pairs, has recently enabled the investigation of the fundamental limit of the rods sensitivity [17], addressing the question if even a single-photon can be discriminated by a human being [229].

In particular, in [17] a single rod toad cell held in a suction pipette is stimulated by photons produced by a SPDC heralded single-photon source. Detection of a photon in the idler path by a SPAD drives an optical shutter in the signal path, which allows only announced photon to address the photoreceptor. The registered amplitude of the electrical signal from the cell presents unambiguous evidence of the detection of some of the heralded photons. The authors also evaluated the quantum efficiency of the rod by the Klyshko two-photon technique to be  $\eta_{\text{rod}} = 0.29(0.04)$ .

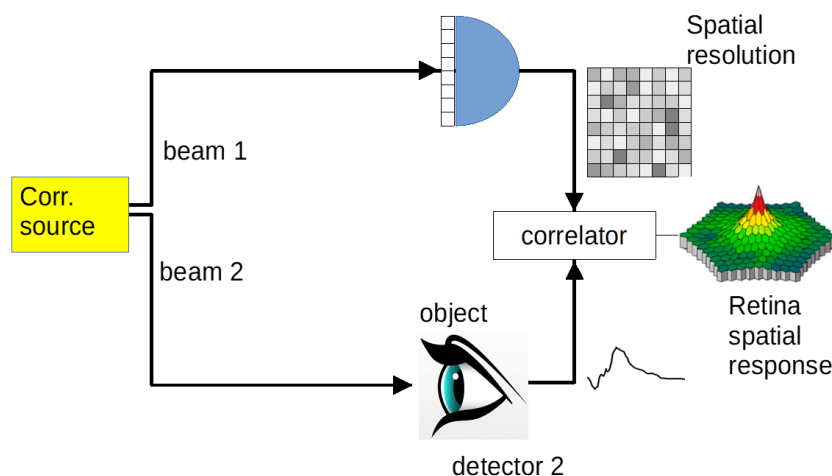


**Figure 11.** Possible QGI scheme applied to retina investigation. The retina is here the bucket detector providing an integrated signal. Using the ghost imaging approach it is possible to reconstruct the spatial mapping of its response.

The first behavioural measurements in which single photons are sent to the human eye were reported in [229]. In that case a sophisticated psychophysical test was used, called the two-alternative forced-choice (2AFC) protocol. In summary, in each trial the subject has to identify a light stimulus (single photon) that can be delivered in two separated temporal bins. The number of correct answers on which time bin contained the photon allows the exclusion of psychophysical false detection. In that case the suppression of the multi-photon component was obtained by post-selection of the trials in which only one photon was detected by a EMCCD used as a spatially multiplexed photon number resolving detector in the idler path. The results show that humans can detect a single-photon incident on the cornea with a probability significantly above chance. Moreover, the probability of detecting a single photon is modulated by the presence of an earlier photon, suggesting a priming process that temporarily enhances the effective gain of the visual system on the timescale of seconds.

Even if single-photon sensitivity of the human eye has been demonstrated, the mechanism of vision at very low-light conditions and the transition to the mesopic regime remains mostly unexplored. This opens up the opportunity to develop a broad new metrological field, which we will refer to as quantum photometry. Indeed, applying new quantum radiometry tools can have a strong impact in understanding the physiological processes involved, eventually supporting vision neurophysiology and research in computer vision as well as the investigation and early detection of pathological conditions. In addition, it must be stressed that the human retina is part of the central nervous system (CNS) which can be directly *in vivo* approached and that many CNS-related disorders (from multiple sclerosis to neurodegenerative disorders) are known to affect the retina as well, making the retina a powerful biomarker both of disease progression and of pharmacological treatments. Daring a little more, QGI and QGS have the potential to be applied to the retina (a sketch is presented in figure 11). Retina spatial and spectral response could be reconstructed by the global evoked electric signal collected with non-invasive skin electrodes, probably the less-invasive approach possible to the

problem of retina spatial mapping and damaged area detection. Furthermore, QGI is expected to be particularly efficient and accurate with respect to standard techniques when faint illumination is used, down to the regime in which few- or even single- photons are detected one by one.

## 6. Final remarks and conclusion

Quantum photonics is considered one of the major future challenges, but also a big opportunity, for the forthcoming quantum industry with respect to innovation and high technology. Therefore, in the near future it is expected that national metrology institutes will be asked, by industries, standardisation bodies and governments, to contribute to standardisation and certification of quantum photonic technologies [230, 231]. The metrological community should be proactive in promoting take-up of metrology in the development of these technologies [232]. Photonics covers transversally a relevant part of the whole field of quantum technologies [233].

- Quantum sensing and metrology (with optical, magneto-optical and optomechanical imaging and sensing techniques, including new metrological standards),
- Quantum communication (with quantum key distribution, with discrete and with continuous variables),
- Quantum simulation (with photonic circuits).

In particular, in this paper we have presented and discussed quantum sensing and metrology techniques exploiting sub-Poissonian photon statistics and non-classical photon number correlations. We have highlighted state of the art non-classical light sources, such as single-photon sources and twin beams, discussing their performance and limitations. We have seen that the non-classical states of light produced by these sources can represent a breakthrough, improving both the spatial resolution and sensitivity of measurements, especially in dim optical power conditions, even though actual techniques are in several cases strongly limited by optical losses. The possibility of reducing the measurement uncertainty opens



itself new research directions in modern optical metrology. Moreover, the development of quantum enhanced optical measurement is also a great opportunity for metrologists related to the above-mentioned demand of characterisation and certification infrastructure for quantum technologies. It is of particular interest, from the radiometric point of view, that absolute light sources with sub-shot-noise performance in the few- and single-photon regime as well as reliable absolute calibration techniques for detectors based on quantum correlation are developed. These future developments of deterministic quantum sources could be disruptive for radiometry and photometry, leading to the realisation of a new type of primary standard and paving the way for a possible redefinition of the unit Candela in terms of number of photons [118]. At the same time, the possibility of investigating biophysical process with these new tools, absolute and accurate, opens new metrological and research fields one example that we have reported here is the study of vision mechanisms at the single-photon level, dubbed quantum photometry.

## Acknowledgments

This work has been supported by EMPIR 14IND05 ‘MIQC2’, EMPIR 17FUN01 ‘BeCOMe’, EMPIR 17FUN06 ‘SIQUEST’ (the EMPIR initiative is co-funded by the EU H2020 and the EMPIR Participating States). IRB and IPD are deeply indebted with Elena Losero for useful suggestions to improve the manuscript.

## References

- [1] Dowling J P and Milburn G J 2013 Quantum technology: the second quantum revolution *Phil. Trans. R. Soc. A* **361** 3655
- [2] O’Brien J L, Furusawa A and Vukovi J 2009 Photonic quantum technologies *Nat. Photon.* **3** 687
- [3] Lo H K, Curty M and Tamaki K 2014 Secure quantum key distribution *Nat. Photon.* **8** 595
- [4] Aasi J *et al* 2013 Enhanced sensitivity of the LIGO gravitational wave detector by using squeezed states of light *Nat. Photon.* **7** 613
- [5] Taylor M A *et al* 2014 Subdiffraction-limited quantum imaging within a living cell *Phys. Rev. X* **4** 011017
- [6] Samantaray N, Ruó-Berchera I, Meda A and Genovese M 2017 Realisation of the first sub shot noise wide field microscope *Light Sci. Appl.* **6** e17005
- [7] Morris P A *et al* 2015 Imaging with a small number of photons *Nat. Commun.* **6** 5913
- [8] Kalashnikov D A, Paterova A V, Kulik S P and Krivitsky L A 2016 Infrared spectroscopy with visible light *Nat. Photon.* **10** 98
- [9] Pooser R C and Lawrie B 2015 Ultrasensitive measurement of microcantilever displacement below the shot-noise limit *Optica* **2** 393
- [10] Zhang Z, Mouradian S, Wong F N C and Shapiro J H 2015 *Phys. Rev. Lett.* **114** 110506
- [11] Genovese M 2016 Real applications of quantum imaging *J. Opt.* **18** 7
- [12] Meda A 2016 Photon-number correlation for quantum enhanced imaging and sensing *J. Opt.* **19** 094002
- [13] Polyakov S V and Migdall A L 2007 High accuracy verification of a correlated-photon-based method for determining photon-counting detection efficiency *Opt. Express* **15** 1390
- [14] Brida G, Degiovanni I P, Genovese M, Rastello M L and Ruó-Berchera I 2010 Detection of multimode spatial correlation in PDC and application to the absolute calibration of a CCD camera *Opt. Express* **18** 20572
- [15] Avella A, Ruó-Berchera I, Degiovanni I P, Brida G and Genovese M 2016 Absolute calibration of an EMCCD camera by quantum correlation, linking photon counting to the analog regime *Opt. Lett.* **41** 1841
- [16] Taylor M A and Bowen W P 2016 Quantum metrology and its application in biology *Phys. Rep.* **615** 1
- [17] Phan N M *et al* 2014 Interaction of fixed number of photons with retinal rod cells *Phys. Rev. Lett.* **112** 213601
- [18] Jacques S L 2013 Optical properties of biological tissues: a review *Phys. Med. Biol.* **58** R37
- [19] Gu M, Li X and Cao Y 2014 Optical storage arrays: a perspective for future big data storage *Light Sci. Appl.* **3** e177
- [20] Kurtsiefer C, Mayer S, Zarda P and Weinfurter H 2000 Stable solid-state source of single photons *Phys. Rev. Lett.* **85** 290
- [21] Zaitsev A M 2000 Vibronic spectra of impurity-related optical centers in diamond *Phys. Rev. B* **61** 12909
- [22] Aharonovich I *et al* 2009 Enhanced single-photon emission in the near infrared from a diamond color center *Phys. Rev. B* **79** 235316
- [23] Migdall A, Polyakov S, Fan J and Bienfang J 2013 Single-photon generation and detection *Experimental Methods in Physical Science* vol 45 (New York: Academic)
- [24] Eisamana M D, Fan J, Migdall A and Polyakov S V 2011 Single-photon sources and detectors *Rev. Sci. Instrum.* **82** 071101
- [25] Pérez-Delgado C A, Pearce M E and Kok P 2012 Fundamental limits of classical and quantum imaging *Phys. Rev. Lett.* **109** 123601
- [26] Thiel C *et al* 2007 Quantum imaging with incoherent photons *Phys. Rev. Lett.* **99** 133603
- [27] Oppel S, Buttner T, Kok P and vonZanthier J 2012 Superresolving multiphoton interferences with independent light sources *Phys. Rev. Lett.* **109** 233603
- [28] Beskrovny V N and Kolobov M I 2005 Quantum limits of super-resolution in reconstruction of optical objects *Phys. Rev. A* **71** 043802
- [29] D’Angelo M, Checkhova M V and Shih Y 2001 Two-photon diffraction and quantum lithography *Phys. Rev. Lett.* **87** 013602
- [30] Distante E, Jezek M and Andersen U L 2013 Deterministic superresolution with coherent states at the shot noise limit *Phys. Rev. Lett.* **111** 033603
- [31] Björk G, Sánchez-Soto L L and Söderholm J 2001 Subwavelength lithography over extended areas *Phys. Rev. A* **64** 013811
- [32] Igarashi R *et al* 2012 Real-time background-free selective imaging of fluorescent nanodiamonds *in vivo* *Nano Lett.* **12** 5726
- [33] Le Sage D *et al* 2013 Optical magnetic imaging of living cells *Nature* **496** 486
- [34] Steinert S *et al* 2013 Magnetic spin imaging under ambient conditions with sub-cellular resolution *Nat. Commun.* **4** 1607
- [35] Dolde F *et al* 2013 Room-temperature entanglement between single defect spins in diamond *Nat. Phys.* **9** 139
- [36] Hell S W and Wichmann J 1994 Breaking the diffraction resolution limit by stimulated emission: stimulated-emission-depletion fluorescence microscopy *J. Opt. Lett.* **19** 780
- [37] Hell S W and Kroug M 1995 Ground-state-depletion fluorescence microscopy: a concept for breaking the diffraction resolution limit *Appl. Phys. B* **60** 495

- [38] Rittweger E, Han K Y, Irvine S E, Eggeling C and Hell S W 2009 STED microscopy reveals crystal colour centres with nanometric resolution *Nat. Photon.* **3** 144
- [39] Giovannetti V, Lloyd S and Maccone L 2011 Advances in quantum metrology *Nat. Photon.* **5** 222
- [40] Demkowicz-Dobrzanski R, Jarzyna M and Koodyski J 2015 Quantum limits in optical interferometry *Prog. Opt.* **60** 345
- [41] Braun D *et al* 2018 Quantum-enhanced measurements without entanglement *Rev. Mod. Phys.* **90** 035006
- [42] Monras A and Paris M G A 2007 Optimal quantum estimation of loss in bosonic channels *Phys. Rev. Lett.* **98** 160401
- [43] Mandel J and Wolf E 1995 *Optical Coherence and Quantum Optics* (Cambridge: Cambridge University Press)
- [44] Davidovich L 1996 Sub-poissonian processes in quantum optics *Rev. Mod. Phys.* **68** 127
- [45] Adesso G, Dell'Anno F, De Siena S, Illuminati F and Souza L A M 2009 Optimal estimation of losses at the ultimate quantum limit with non-Gaussian states *Phys. Rev. A* **79** 040305
- [46] Monras A and Illuminati F 2011 Measurement of damping and temperature: precision bounds in Gaussian dissipative channels *Phys. Rev. A* **83** 012315
- [47] Giovannetti V, Lloyd S and Maccone L 2004 Quantum-enhanced measurements: beating the standard quantum limit *Science* **306** 1330
- [48] Genovese M 2005 Research on hidden variable theories: a review of recent progresses *Phys. Rep.* **413** 319
- [49] Giustina M *et al* 2015 Significant-loophole-free test of bells theorem with entangled photons *Phys. Rev. Lett.* **115** 250401
- [50] Shalm L K *et al* 2015 Strong loophole-free test of local realism *Phys. Rev. Lett.* **115** 250402S
- [51] Einstein A, Podolsky B and Rosen N 1935 Can quantum-mechanical description of physical reality be considered complete? *Phys. Rev.* **47** 777
- [52] Huelga S F, Macchiavello C, Pellizzaro T and Ekert A K 1997 Improvement of frequency standards with quantum entanglement *Phys. Rev. Lett.* **79** 3865
- [53] Boto A *et al* 2000 Quantum interferometric optical lithography: exploiting entanglement to beat the diffraction limit *Phys. Rev. Lett.* **85** 2733
- [54] Holland M J and Burnett K 1993 Interferometric detection of optical phase shifts at the Heisenberg limit *Phys. Rev. Lett.* **71** 1355
- [55] Campos R A, Gerry C C and Benmoussa A 2003 Optical interferometry at the Heisenberg limit with twin Fock states and parity measurements *Phys. Rev. A* **68** 023810
- [56] Slussarenko S *et al* 2017 Unconditional violation of the shot-noise limit in photonic quantum metrology *Nat. Photon.* **11** 700
- [57] Jachura M, Chrapkiewicz R, Demkowicz-Dobrzanski R, Wasilewski W and Banaszek K 2016 Mode engineering for realistic quantum-enhanced interferometry *Nat. Commun.* **7** 11411
- [58] Demkowicz-Dobrzanski R, Koodyski J and Gu M 2012 The elusive Heisenberg limit in quantum-enhanced metrology *Nat. Commun.* **3** 1063
- [59] Giovannetti V and Maccone L 2012 Sub-heisenberg estimation strategies are ineffective *Phys. Rev. Lett.* **108** 210404
- [60] Tsang M 2013 Quantum metrology with open dynamical systems *New J. Phys.* **15** 073005
- [61] Vitelli C, Spagnolo N, Sciarrino F and De Martini F 2009 Amplification of polarization NOON states *J. Opt. Soc. Am. B* **5** 892
- [62] Ono T, Okamoto R and Takeuchi S 2013 An entanglement-enhanced microscope *Nat. Commun.* **4** 2426
- [63] Israel Y, Rosen S and Silberberg Y 2014 Supersensitive polarization microscopy using NOON states of light *Phys. Rev. Lett.* **112** 103604
- [64] Wolfgramm F, Vitelli C, Beduini F A, Godbout N and Mitchell M W 2013 Entanglement-enhanced probing of a delicate material system *Nat. Photon.* **7** 28
- [65] Crespi A *et al* 2012 Measuring protein concentration with entangled photons *Appl. Phys. Lett.* **100** 233704
- Matthews C F J, Alberto P, Bonneau D and OBrien J L 2011 Heralding two-photon and four-photon path entanglement on a chip *Phys. Rev. Lett.* **107** 163602
- [66] Olivares S, Popovic M and Paris M G A 2016 Phase estimation with squeezed single photons *Quantum Meas. Quantum Metr.* **3**
- [67] Andersen U, Gehring T, Marquardt C and Leuchs G 2016 30 years of squeezed light generation *Phys. Scr.* **91** 053001
- [68] Schnabel R 2017 Squeezed states of light and their applications in laser interferometers *Phys. Rep.* **684** 1
- [69] Caves C M 1981 Quantum-mechanical noise in an interferometer *Phys. Rev. D* **23** 1708
- [70] Abadie J *et al* 2011 A gravitational wave observatory operating beyond the quantum shot-noise limit *Nat. Phys.* **7** 962
- [71] Taylor M A, Janousek J, Knittel D J, Hage B, Bachor H A and Bowen W P 2013 Biological measurement beyond the quantum limit *Nat. Photon.* **7** 229
- [72] Treps N, Grosse N, Bowen W P, Fabre C, Bachor H A and Lam P K 2003 A quantum laser pointer *Science* **301** 940
- [73] Ruo-Berchera I, Degiovanni I P, Olivares S and Genovese M 2013 Quantum light in coupled interferometers for quantum gravity tests *Phys. Rev. Lett.* **110** 213601
- [74] Souza L A M, Dhar H S, Bera M N, Liuzzo-Scorpo P and Adesso G 2015 Gaussian interferometric power as a measure of continuous-variable non-Markovianity *Phys. Rev. A* **92** 052122
- [75] Kolobov M I 2007 *Quantum Imaging* (New York: Springer)
- [76] Zel'Dovich Y B and Klyshko D N 1969 Fields statistics in parametric fluorescence process *Sov. Phys.—JETP* **9** 40
- [77] Burnham D C and Weinberg D L 1970 Observation of simultaneity in parametric production of optical photon pairs *Phys. Rev. Lett.* **25** 84
- [78] Ruo-Berchera I 2009 Theory of PDC in a continuous variables framework and its applications to the absolute calibration of photo-detectors *Adv. Sci. Lett.* **2** 407
- [79] Jedrkiewicz O *et al* 2004 Detection of sub-shot-noise spatial correlation in high-gain parametric down conversion *Phys. Rev. Lett.* **93** 243601
- [80] Mosset A, Devaux F and Lantz E 2005 Spatially noiseless optical amplification of images *Phys. Rev. Lett.* **94** 223603
- [81] Blanchet J L, Devaux F, Furfaro L and Lantz E 2008 Measurement of sub-shot-noise correlations of spatial fluctuations in the photon-counting regime *Phys. Rev. Lett.* **101** 233604
- [82] Bondani M, Allevi A, Zambra G, Paris M G A and Andreoni A 2007 Sub-shot-noise photon-number correlation in a mesoscopic twin beam of light *Phys. Rev. A* **76** 013833
- [83] Perina J J, Hamar M, Michalek V and Haderka O 2012 Photon-number distributions of twin beams generated in spontaneous parametric down-conversion and measured by an intensified CCD camera *Phys. Rev. A* **85** 023816
- [84] Iskhakov T S *et al* 2016 Heralded source of bright multi-mode mesoscopic sub-Poissonian light *Opt. Lett.* **41** 2149
- [85] Iskhakov T S, Usenko V C, Filip R, Chekhova M V and Leuchs G 2016 Low-noise macroscopic twin beams *Phys. Rev. A* **93** 043849

- [86] Ishkakov T S, Chekhova M V and Leuchs G 2009 Generation and direct detection of broadband mesoscopic polarization-squeezed vacuum *Phys. Rev. Lett.* **102** 183602
- [87] Tapster P R, Seward S F and Rarity J G 1991 Sub-shot-noise measurement of modulated absorption using parametric down-conversion *Phys. Rev. A* **44** 3266
- [88] Lamperti M, Allevi A and Bondani M 2014 Generation of sub-Poissonian non-Gaussian states from multimode twin beams by photon-number-resolving detectors *Int. J. Quantum Inf.* **12** 1461017
- [89] Heidmann A, Horowicz R J, Reynaud S, Giacobino E and Fabre C 1987 Observation of quantum noise reduction on twin laser beams *Phys. Rev. Lett.* **59** 2555
- [90] Mertz J, Heidmann A, Fabre C, Giacobino E and Reynaud S 1990 Observation of high-intensity sub-Poissonian light using an optical parametric oscillator *Phys. Rev. Lett.* **64** 2897
- [91] Agafonov I N *et al* 2011 Absolute calibration of photodetectors: photocurrent multiplication versus photocurrent subtraction *Opt. Lett.* **36** 1329
- [92] Brida G *et al* 2009 Measurement of sub shot-noise spatial correlations without background subtraction *Phys. Rev. Lett.* **102** 213602
- [93] Glorieux Q, Guidoni L, Guibal S, Likforman J P and Coudreau T 2011 Quantum correlations by four-wave mixing in an atomic vapor in a nonamplifying regime: quantum beam splitter for photons *Phys. Rev. A* **84** 053826
- [94] Embrey C S, Turnbull M T, Petrov P G and Boyer V 2015 Observation of localized multi-spatial-mode quadrature squeezing *Phys. Rev. X* **5** 031004
- [95] Cao L *et al* 2017 Experimental observation of quantum correlations in four-wave mixing with a conical pump *Opt. Lett.* **42** 1201
- [96] Boyer V, Marino A M, Pooser R C and Lett P D 2008 Entangled images from four-wave mixing *Science* **321** 544
- [97] Jakeman E and Rarity J G 1986 The use of pair production processes to reduce quantum noise in transmission measurements *Opt. Commun.* **59** 219
- [98] Hayat M M, Joobeur A and Saleh B E 1999 Reduction of quantum noise in transmittance estimation using photon-correlated beams *J. Opt. Soc. Am.* **16** 348
- [99] Moreau P A *et al* 2017 Demonstrating an absolute quantum advantage in direct absorption measurement *Sci. Rep.* **7** 6256
- [100] Losero E, Ruó-Berchera I, Meda A, Avella A and Genovese M 2018 Unbiased estimation of an optical loss at the ultimate quantum limit with twin-beams *Sci. Rep.* **8** 7431
- [101] Abouraddy A F, Toussaint K C Jr, Sergienko A V, Saleh B E A and Teich M C 2001 *Opt. Lett.* **26** 1717
- [102] Toussaint K C Jr, Di Giuseppe G, Bycenski K J, Sergienko A V, Saleh B E A and Teich M C 2004 *Phys. Rev. A* **70** 023801
- [103] Lopaeva E D *et al* 2013 Experimental realization of quantum illumination *Phys. Rev. Lett.* **110** 153603
- [104] Clark J B, Zhou Z, Glorieux Q, Marino M A and Lett P D 2012 Imaging using quantum noise properties of light *Opt. Express* **20** 17050
- [105] Pirandola S 2011 Quantum reading of a classical digital memory *Phys. Rev. Lett.* **106** 090504
- [106] Lawrie B J, Evans P G and Pooser R C 2013 Extraordinary optical transmission of multimode quantum correlations via localized surface plasmons *Phys. Rev. Lett.* **110** 156802
- [107] Pooser R C and Lawrie B 2016 Plasmonic trace sensing below the photon noise limit *ACS Photon.* **3** 8
- [108] Corzo N V, Marino A M, Jones K M and Lett P D 2012 Noiseless optical amplifier operating on hundreds of spatial modes *Phys. Rev. Lett.* **109** 043602
- [109] Adenier G *et al* 2016 Realization of a twin beam source based on four-wave mixing in Cesium *Int. J. Quantum Inf.* **14** 1640014
- [110] Brambilla E, Caspani L, Jedrkiewicz O, Lugiato L A and Gatti A 2008 High-sensitivity imaging with multi-mode twin beams *Phys. Rev. A* **77** 053807
- [111] Brida G, Genovese M and Berchera I R 2010 Experimental realization of sub-shot-noise quantum imaging *Nat. Photon.* **4** 227
- [112] Brida G, Genovese M, Meda A and Ruó-Berchera I 2011 Experimental quantum imaging exploiting multimode spatial correlation of twin beams *Phys. Rev. A* **83** 033811
- [113] Belinskii A and Klyshko D 1994 Two-photon optics: diffraction, holography, and transformation of two-dimensional signals *Sov. Phys.—JETP* **78** 259
- [114] Pittman T B, Shih Y H, Strekalov D V and Sergienko A V 1995 Optical imaging by means of two-photon quantum entanglement *Phys. Rev. A* **52** R3429–32
- [115] Gatti A, Brambilla E, Bache M and Lugiato L A 2004 Correlated imaging quantum and classical *Phys. Rev. A* **70** 013802
- [116] Erkmen B I and Shapiro J H 2009 Signal-to-noise ratio of Gaussian-state ghost imaging *Phys. Rev. A* **79** 023833
- [117] Brida G *et al* 2011 Systematic analysis of signal-to-noise ratio in bipartite ghost imaging with classical and quantum light *Phys. Rev. A* **83** 063807
- [118] Zwinkels J C, Ikonen E, Fox N P, Ulm G and Rastello M L 2010 Photometry, radiometry and the candela: evolution in the classical and quantum world *Metrologia* **47** R15
- [119] Meda A *et al* 2014 Absolute calibration of a charge-coupled device camera with twin beams *Appl. Phys. Lett.* **105** 101113
- [120] Haderka O, Perina J, Michalek V and Hamar M 2014 Absolute spectral calibration of an intensified CCD camera using twin beams *J. Opt. Soc. Am. B* **31** 10
- [121] Qi L, Just F, Leuchs G and Chekhova M V 2016 Autonomous absolute calibration of an ICCD camera in single-photon detection regime *Opt. Express* **24** 26444
- [122] Lounis B and Orrit M 2005 Single-photon sources *Rep. Prog. Phys.* **68** 1129
- [123] Scheel S 2009 Single-photon sources—an introduction *J. Mod. Opt.* **56** 141
- [124] Polyakov S and Migdall A 2009 Quantum radiometry *J. Mod. Opt.* **56** 1045 (and references therein)
- [125] Lundeen J S *et al* 2009 Tomography of quantum detectors *Nat. Phys.* **5** 27
- [126] Avella A *et al* 2011 Self consistent, absolute calibration technique for photon number resolving detectors *Opt. Express* **19** 23249
- [127] Brida G *et al* 2012 Quantum characterization of superconducting photon counters *New J. Phys.* **14** 085001
- [128] Brida G *et al* 2012 Ancilla-assisted calibration of a measuring apparatus *Phys. Rev. Lett.* **108** 253601
- [129] Degen C L, Reinhard F and Cappellaro P 2017 Quantum sensing *Rev. Mod. Phys.* **89** 035002
- [130] Rodiek B *et al* 2017 Experimental realization of an absolute single-photon source based on a single nitrogen vacancy center in a nanodiamond *Optica* **4** 71
- [131] Vaigu A, Porrovecchio G, Chu X-L, Lindner S, Smid M, Manninen A, Becher C, Sandoghdar V, Gotzinger S and Ikonen E 2017 Experimental demonstration of a predictable single photon source with variable photon flux *Metrologia* **54** 218
- [132] Müller T, Aharonovich I, Wang Z, Yuan X, Castelletto S, Prawer S and Atatüre M 2012 Phonon-induced dephasing of chromium color centers in diamond *Phys. Rev. B* **86** 195210
- [133] Brokmann X, Coolen L, Dahan M and Hermier J P 2004 Measurement of the radiative and nonradiative decay



- rates of single CdSe nanocrystals through a controlled modification of their spontaneous emission *Phys. Rev. Lett.* **93** 107403
- [134] Gerard J M *et al* 1998 Enhanced spontaneous emission by quantum boxes in a monolithic optical microcavity *Phys. Rev. Lett.* **81** 1110
- [135] Lee K G *et al* 2011 A planar dielectric antenna for directional single-photon emission and near-unity collection efficiency *Nat. Photon.* **5** 166
- [136] Claudon J *et al* 2010 A highly efficient single photon source based on a quantum dot in a photonic nanowire *Nat. Photon.* **4** 174
- [137] Reimer M E *et al* 2012 Bright single photon sources in bottom up tailored nanowires *Nat. Commun.* **3** 737
- [138] Munsch M *et al* 2013 Dielectric GaAs antenna ensuring an efficient broadband coupling between an InAs quantum dot and a Gaussian optical beam *Phys. Rev. Lett.* **110** 177402
- [139] Gatto Monticone D 2014 Single-photon emitters based on NIR colour centres in diamond coupled with solid immersion lenses *Int. J. Quantum Inf.* **12** 1560011
- [140] Ates S, Sapienza L, Davanco M, Badolato A and Srinivasan K 2012 Bright single photon emission from a quantum dot in a circular bragg grating microcavity *IEEE J. Sel. Top. Quantum Electron.* **18** 1711–21
- [141] Riedel D *et al* 2014 Low-loss broadband antenna for efficient photon collection from a coherent spin in diamond *Phys. Rev. Appl.* **2** 064011
- [142] Checcucci S *et al* 2017 Beaming light from a quantum emitter with a planar optical antenna *Light Sci. Appl.* **6** e16245
- [143] Loredó J C *et al* 2016 Scalable performance in solid-state single-photon sources *Optica* **3** 433
- [144] Somaschi N *et al* 2016 Near-optimal single-photon sources in the solid state *Nat. Photon.* **10** 340
- [145] Chu X-L, Gotzingerand S and Sandoghdar V 2017 A single molecule as a high-fidelity photon gun for producing intensity-squeezed light *Nat. Photon.* **11** 58
- [146] Brida G, Degiovanni I P, Genovese M, Migdall A, Piacentini F, Polyakov S V and Ruo Berchera I 2011 Experimental realization of a low-noise heralded single-photon source *Opt. Express* **19** 1484
- [147] Krapick S, Herrmann H, Quiring V, Brecht B, Suche H and Silberhorn C 2013 An efficient integrated two-color source for heralded single photons *New J. Phys.* **15** 033010
- [148] Brida G *et al* 2012 An extremely low-noise heralded single-photon source: A breakthrough for quantum technologies *Appl. Phys. Lett.* **101** 221112
- [149] Whittaker R, Erven C, Neville A, Berry M, O'Brien J L, Cable H and Matthews J C F 2017 Absorption spectroscopy at the ultimate quantum limit from single-photon states *New J. Phys.* **19** 023013
- [150] Sabines-Chesterking J 2017 Sub-shot-noise transmission measurement enabled by active feed-forward of heralded single photons *Phys. Rev. Appl.* **8** 014016
- [151] Schwartz O and Oron D 2012 Improved resolution in fluorescence microscopy using quantum correlations *Phys. Rev. A* **85** 033812
- [152] Schwartz O, Levitt J M, Tenne R, Itzhakov S, Deutsch Z and Oron D 2013 Superresolution microscopy with quantum emitters *Nano Lett.* **13** 5832
- [153] Gatto Monticone D *et al* 2014 Beating the Abbe diffraction limit in confocal microscopy via nonclassical photon statistics *Phys. Rev. Lett.* **113** 143602
- [154] Classen A, von Zanthier J, Scully M O and Agarwal G S 2017 Superresolution via structured illumination quantum correlation microscopy *Optica* **4** 580
- [155] Israel Y, Tenne R, Oron D and Silberberg Y 2017 Quantum correlation enhanced super-resolution localization microscopy enabled by a fibre bundle camera *Nat. Commun.* **8** 14786
- [156] Tsang M, Nair R and Lu X M 2016 Quantum theory of superresolution for two incoherent optical point sources *Phys. Rev. X* **6** 031033
- [157] Helstrom C W 1976 *Quantum Detection and Estimation Theory* (New York: Academic)
- [158] Lupo C and Pirandola S 2016 Ultimate precision bound of quantum and subwavelength imaging *Phys. Rev. Lett.* **117** 190802
- [159] Nair R and Tsang M 2016 Far-field superresolution of electromagnetic source at the quantum limit *Phys. Rev. Lett.* **117** 190801
- [160] Rehacek J, Paur M, Stoklasa B, Hradil Z and Sanchez-Soto L L 2017 Optimal measurements for resolution below the Rayleigh limit *Opt. Lett.* **42** 231
- [161] Yang F, Nair R, Tsang M, Simon C and Lvovsky A 2017 Fisher information for far-field linear optical superresolution via homodyne and heterodyne detection in a higher-order local oscillator mode *Phys. Rev. A* **96** 063829
- [162] Tang Z S, Durak K and Ling A 2016 Fault tolerant and finite-error localization for point-emitter within the diffraction limit *Opt. Express* **24** 22004
- [163] Nair R and Tsang M 2016 Interferometric superlocalization of two incoherent optical point sources *Opt. Express* **24** 3604
- [164] Yang F, Taschilina A, Moiseev E S, Simon C and Lvovsky A 2016 Far-field optical superresolution via heterodyne detection in a high-order local oscillator mode *Optica* **3** 1148
- [165] Tham W K, Ferretti H and Steinberg A M 2017 Beating Rayleigh's curse by imaging using phase information *Phys. Rev. Lett.* **118** 070801
- [166] Paur M, Stoklasa B, Hradil Z, Sanchez-Soto L L and Rehacek J 2016 Achieving the ultimate optical resolution *Optica* **3** 1144
- [167] Paris M G A 2009 Quantum estimation for quantum technology *Int. J. Quantum Inf.* **7** 125
- [168] Cole R 2015 Live-cell imaging; the cell's perspective *Cell Adhes. Migration* **8** 5
- [169] Barnett S M, Fabre C and Maitre A 2003 Ultimate quantum limits for resolution of beam displacements *Eur. Phys. J. D* **22** 513
- [170] Fabre C, Fouet J B and Maitre A 2000 Quantum limits in the measurement of very small displacements in optical images *Opt. Lett.* **25** 76
- [171] Treps N, Andersen U, Buchler B, Lam P K, Maitre A, Bachor H A and Fabre C 2002 Surpassing the standard quantum limit for optical imaging using nonclassical multimode light *Phys. Rev. Lett.* **88** 203601
- [172] Lyons K, Pang S, Kwiat P G and Jordan A N 2016 Precision optical displacement measurements using biphotons *Phys. Rev. A* **93** 043841
- [173] Toninelli E *et al* 2017 Sub-shot-noise shadow sensing with quantum correlations *Opt. Express* **25** 21827
- [174] Gatti A, Brambilla E, Bache M and Lugiato L A 2004 Ghost imaging with thermal light: comparing entanglement and classical correlation *Phys. Rev. Lett.* **93** 093602
- [175] Bache M, Brambilla E, Gatti A and Lugiato L A 2004 Ghost imaging using homodyne detection *Phys. Rev. A* **70** 023823
- [176] Shapiro J H and Boyd R W 2012 The physics of ghost imaging *Quantum Inf. Process.* **11** 949
- [177] Bennink R S, Bentley S J and Boyd R W 2002 Two-photon coincidence imaging with a classical source *Phys. Rev. Lett.* **89** 113601
- [178] Ferri F, Magatti D, Gatti A, Bache M, Brambilla E and Lugiato L A 2005 High-resolution ghost image and ghost

- diffraction experiments with thermal light *Phys. Rev. Lett.* **94** 183602
- [179] Valencia A, Scarcelli G, D'Angelo M and Shih Y 2005 Two-photon imaging with thermal light *Phys. Rev. Lett.* **94** 063601
- [180] Chen X, Agafonov I N, Luo K, Liu Q, Xian R, Chekhova M V and Wu L 2010 High-visibility, high-order lensless ghost imaging with thermal light *Opt. Lett.* **35** 1166
- [181] Zhai Y, Chen X, Zhang D and Wu L 2005 Two-photon interference with true thermal light *Phys. Rev. A* **72** 043805
- [182] Liu X, Chen X, Yao X, Yu W, Zhai G and Wu L 2014 Lensless ghost imaging with sunlight *Opt. Lett.* **39** 2314
- [183] Hartmann S, Molitor A and Elsassner W 2015 Ultrabroadband ghost imaging exploiting optoelectronic amplified spontaneous emission and two-photon detection *Opt. Lett.* **40** 5770
- [184] Puddu E, Andreoni A, Degiovanni I P, Bondani M and Castelletto S 2007 Ghost imaging with intense fields from chaotically seeded parametric downconversion *Opt. Lett.* **32** 1132
- [185] Shapiro J H 2008 Computational ghost imaging *Phys. Rev. A* **78** 061802
- [186] Bromberg Y, Katz O and Silberberg Y 2009 *Phys. Rev. A* **79** 053840
- [187] Katz O, Bromberg Y and Silberberg Y 2009 Compressive ghost imaging *Appl. Phys. Lett.* **95** 131110
- [188] Bina M, Magatti D, Molteni M, Gatti A, Lugiatto L A and Ferri F 2013 Backscattering differential ghost imaging in turbid media *Phys. Rev. Lett.* **110** 083901
- [189] Meyers R, Deacon K S and Shih Y 2008 Ghost-imaging experiment by measuring reflected photons *Phys. Rev. A* **77** 041801
- [190] Welsh S S, Edgar M P, Bowman R, Jonathan P, Sun B and Padgett M J 2013 Fast full-color computational imaging with single-pixel detectors *Opt. Express* **21** 23068
- [191] Duan D, Du S and Xia Y 2013 Multiwavelength ghost imaging *Phys. Rev. A* **88** 053842
- [192] Sun B *et al* 2013 3D computational imaging with single-pixel detectors *Science* **340** 844
- [193] Chan K W C, O'Sullivan M N and Boyd R W 2010 Optimization of thermal ghost imaging: high-order correlations versus background subtraction *Opt. Express* **18** 5562
- [194] Allevi A, Olivares S and Bondani M 2012 Measuring high-order photon-number correlations in experiments with multimode pulsed quantum states *Phys. Rev. A* **85** 063835
- [195] Yu W *et al* 2014 Adaptive compressive ghost imaging based on wavelet trees and sparse representation *Opt. Exp.* **22** 7133
- [196] Moreau P A, Toninelli E, Gregory T and Padgett M J 2017 Ghost imaging using optical correlations *Laser Photon. Rev.* **12** 1700143
- [197] Dixon P B *et al* 2011 Quantum ghost imaging through turbulence *Phys. Rev. A* **83** 051803
- [198] Gong W and Han S 2011 Correlated imaging in scattering media *Opt. Lett.* **36** 394
- [199] Meyers R E, Deacon K S, Tunick A D and Shih Y 2012 Virtual ghost imaging through turbulence and obscurants using Bessel beam illumination *Appl. Phys. Lett.* **100** 061126
- [200] Rubin M H and Shih Y 2008 Resolution of ghost imaging for nondegenerate spontaneous parametric down-conversion *Phys. Rev. A* **78** 033836
- [201] Chan K W C, O'Sullivan M N and Boyd R W 2009 Two-color ghost imaging *Phys. Rev. A* **79** 033808
- [202] Karmakar S and Shih Y 2010 Observation of two-color ghost imaging *Proc. SPIE* **7702** 770204R
- [203] Aspden R S *et al* 2015 Photon-sparse microscopy: visible light imaging using infrared illumination *Optica* **2** 1049
- [204] Meda A, Caprile A, Avella A, Ruo Berchera I, Degiovanni I P, Magni A and Genovese M 2015 Magneto-optical imaging technique for hostile environments: the ghost imaging approach *Appl. Phys. Lett.* **106** 262405
- [205] Kalashnikov D A, Pan Z, Kuznetsov A I and Krivitsky L A 2014 Quantum spectroscopy of plasmonic nanostructures *Phys. Rev. X* **4** 011049
- [206] Scarcelli G, Valencia A, Gompers S and Shih Y 2003 Remote spectral measurement using entangled photons *Appl. Phys. Lett.* **83** 5560
- [207] Yabushita A and Kobayashi T 2004 Spectroscopy by frequency-entangled photon pairs *Phys. Rev. A* **69** 013806
- [208] Slattery O *et al* 2013 Frequency correlated biphoton spectroscopy using tunable upconversion detector *Laser Phys. Lett.* **10** 075201
- [209] Janassek P, Blumenstein S and Elsassner W 2018 Ghost spectroscopy with classical thermal light emitted by a superluminescent diode *Phys. Rev. Appl.* **9** 021001
- [210] Chekhova M V and Ou Z Y 2016 Nonlinear interferometers in quantum optics *Adv. Opt. Photon.* **8** 104
- [211] Lemos G B *et al* 2014 Quantum imaging with undetected photons *Nature* **512** 409
- [212] Hudelist F *et al* 2014 Quantum metrology with parametric amplifier-based photon correlation interferometers *Nat. Commun.* **5** 3049
- [213] Manceau M, Leuchs G, Khalili F and Chekhova M 2017 Detection loss tolerant supersensitive phase measurement with an SU(1,1) interferometer *Phys. Rev. Lett.* **119** 223604
- [214] Chen B *et al* 2015 Atom-light hybrid interferometer *Phys. Rev. Lett.* **115** 043602
- [215] Lloyd S 2008 Enhanced sensitivity of photodetection via quantum illumination *Science* **321** 1463
- [216] Tan S H, Erkmen B I, Giovannetti V, Guha S, Lloyd S, Maccone L, Pirandola S and Shapiro J H 2008 Quantum illumination with Gaussian states *Phys. Rev. Lett.* **101** 253601
- [217] Shapiro J H and Lloyd S 2009 Quantum illumination versus coherent-state target detection *New J. Phys.* **11** 063045
- [218] Lopaeva E D, Ruo-Berchera I, Olivares S, Brida G, Degiovanni I P and Genovese M 2014 A detailed description of the experimental realization of a quantum illumination protocol *Phys. Scr. T* **160** 014026
- [219] Ragy S, Ruo-Berchera I, Degiovanni I P, Olivares S, Paris M G A, Adesso G and Genovese M 2014 Quantifying the source of enhancement in experimental continuous variable quantum illumination *J. Opt. Soc. Am. B* **31** 2045
- [220] Guha S and Erkmen B I 2009 Gaussian-state quantum-illumination receivers for target detection *Phys. Rev. A* **80** 052310
- [221] Zhuang Q, Zhang Z and Shapiro J H 2017 Quantum illumination for enhanced detection of Rayleigh-fading targets *Phys. Rev. A* **96** 020302
- [222] Zhuang Q *et al* 2017 Optimum mixed-state discrimination for noisy entanglement-enhanced sensing *Phys. Rev. Lett.* **118** 040801
- [223] Zhang S L, Guo J S, Bao W S, Shi J H, Jin C H, Zou X B and Guo G C 2014 Quantum illumination with photon-subtracted continuous-variable entanglement *Phys. Rev. A* **89** 062309
- [224] Barzanjeh S, Guha S, Weedbrook C, Vitali D, Shapiro J H and Pirandola S 2015 Microwave quantum illumination *Phys. Rev. Lett.* **114** 080503



- [225] Shapiro J H 2009 Defeating passive eavesdropping with quantum illumination *Phys. Rev. A* **80** 022320
- [226] Zhang Z, Tengner M, Zhong T, Wong F N C and Shapiro J H 2013 Entanglements benefit survives an entanglement-breaking channel *Phys. Rev. Lett.* **111** 010501
- [227] Rieke F *et al* 1998 Single-photon detection by rod cells of the retina *Rev. Mod. Phys.* **70** 1027
- [228] Hecht S, Schlaer S and Pirenne M 1942 Energy, quanta and vision *J. Gen. Physiol.* **25** 819
- [229] Tinsley J N *et al* 2016 Direct detection of a single photon by humans *Nat. Commun.* **7** 12172
- [230] Langer T and Lenhart G 2009 Standardization of quantum key distribution and the ETSI standardization initiative ISG-QKD *New J. Phys.* **11** 055051
- [231] Alleaume R *et al* 2014 Worldwide standardization activity for quantum key distribution *IEEE Globecom Workshops (GC Wkshps, Austin, TX)* p 656
- [232] Rastello M L *et al* 2014 Metrology for industrial quantum communications: the MIQC project *Metrologia* **51** S267
- [233] Acin A *et al* 2018 The quantum technologies roadmap: a european community view *New J. Phys.* **20** 080201